

AD621250

RADC-TR-65-254  
Final Report



# ENERGY CONVERSION TECHNIQUES FOR MICROWAVE GENERATION

M. C. Pease  
Stanford Research Institute

TECHNICAL REPORT NO. RADC-TR-65-254  
August 1965

OCT 1 1965  
RADC  
TR-65-254

Techniques Branch  
Rome Air Development Center  
Research and Technology Division  
Air Force Systems Command  
Griffiss Air Force Base, New York

CLEARINGHOUSE FOR FEDERAL SCIENTIFIC AND TECHNICAL INFORMATION			
Hardcopy	Microfiche		
\$4.00	\$0.75	105 pp	00
ARCHIVE COPY			

# ENERGY CONVERSION TECHNIQUES FOR MICROWAVE GENERATION

M. C. Pease  
Stanford Research Institute

## FOREWORD

This report was prepared by Stanford Research Institute under Contract No. AF30(602)-3368, Project 4506, Task 450603.

RADC project engineer was Mr. F. Armstrong (EMATP).

This report covers work conducted from 30 March 1964 to 15 May 1965.

At Stanford Research Institute the project supervisor is Dr. Philip Rice, the executive director is Jerre D. Noe. SRI report number is 4913.

This technical report has been reviewed and is approved.

*Fred M. Armstrong*  
Approved: FRED M. ARMSTRONG  
Project Engineer

*Thomas S. Bond, Jr.*  
Approved: THOMAS S. BOND, JR.  
Colonel, USAF  
Chief, Surveillance  
and Control Division

FOR THE COMMANDER:

*Irving J. Gabelman*  
IRVING J. GABELMAN  
Chief, Advanced Studies Group

## ABSTRACT

The purpose of this contract was the study and evaluation of the feasibility of using unconventional methods for the generation of high-power short pulses of microwave energy. For this purpose, converters were studied, using spark gaps operating in various types of microwave structures.

In Section II-A, the general design principles that have emerged from this study are discussed in considerable detail. In Section II-B, it is recognized that the use of spark gaps for RF generation is generically related to the devices used by early workers, and to certain devices currently being studied for sub-microwave operation. A survey of some of the more notable steps in the historical development of such devices is included. In Section II-C, the actual work done under this contract is described in some detail, and the evidence confirming the principles detailed in Section II-A is recounted. In Section III, detailed recommendations for further work are given.

The work, in general, demonstrates that spark gaps can be used for the generation of short (e.g., 100 periods) pulses of microwave energy. It also demonstrates that this method of generating power does require very careful attention to the integrated design of the spark gap and its associated microwave and driving circuitry. The interactions between the spark gap and both the microwave circuitry and the driving circuitry are, in some cases, quite subtle. At this stage in the understanding of the process, it is not sufficient to study the different components separately. It is, instead, of paramount importance to study in detail the performance of the system as a functioning whole.

It is concluded that the use of spark gaps for the generation of short pulses at microwave frequencies is well worth further exploration.

## TABLE OF CONTENTS

Contents	Page
I INTRODUCTION	1
II TECHNICAL DISCUSSION	5
A. General Principles	5
1. Switching Time	5
2. Hertz Effect	7
3. Multiple Spark Gaps	12
a. Parallel Operation	12
b. Series Operation	16
4. Electrode Shape	20
5. Discharge Atmosphere	21
6. Distributed Storage	23
B. Historical Notes and Survey	27
1. Discharge Oscillators	27
2. Coupling Circuits	32
3. Spark Gaps	35
C. Experiments	35
1. Mod I	35
2. Mod II	47
3. Mod III	61
4. Mod IV, Preliminary Design and Measurements	67
5. Supplementary Spark-Gap Studies	76
III CONCLUSIONS AND RECOMMENDATIONS	87
APPENDIX A--ANNOTATED BIBLIOGRAPHY OF SPARK-GAP TECHNOLOGY	91
REFERENCES	93

# LIST OF ILLUSTRATIONS

Page	Illustration	Page
1	Fig. 1 Ideal Hertz Oscillator	9
5	Fig. 2(a) Multiple Generators in Parallel without Synchroniza- tion	14
5	Fig. 2(b) Equivalent Circuit	14
5	Fig. 3 Series Connection of Two Gaps	17
7	Fig. 4 Simplified Circuit of Coaxial Generator	25
2	Fig. 5 Essentials of Classical Meter-Wave Generators	28
2	Fig. 6 Essentials of Classical Centimeter-Wave Generators	28
6	Fig. 7 Spark-Gap Ring Transmitter of Dolphin and Wickersham	31
0	Fig. 8 Circuit of Hellar and Holter	33
1	Fig. 9 Schematic Representation of Mod I Converter	36
3	Fig. 10 Proposed Mercury-Wetted Vibratory Spark-Gap Design	41
7	Fig. 11 Output Pulse Envelope of Mod I Converter	43
7	Fig. 12 RF Waveform (voltage vs. time) at Start of Output (Time scale: 1.0 nanosec./div)	45
2	Fig. 13 Switch Current Waveforms	46
5	Fig. 14 Waveguide Exciter for Mod II Converter	48
5	Fig. 15 Photograph of Mercury-Wetted Reed Switch (Clare RP 5430)	48
7	Fig. 16 Components of Mod II Extractor	50
1	Fig. 17 Schematic Diagram of Mod II Extractor and Test Equipment	52
6	Fig. 18 Voltage Envelope of Forward-Wave Output Pulse ( $\approx 3^\circ$ ) (Hewlett-Packard 185B Sampling Oscilloscope)	54
7	Fig. 19 RF Waveform of Forward-Wave Output Pulse ( $\approx 3^\circ$ ) (Sampling Oscilloscope)	54
1	Fig. 20 Variation of Output Power with Angle of Tilt for the Forward-Wave Pulse	55

# LIST OF ILLUSTRATIONS CONT'D

Illustration		Page
Fig. 21	Voltage Envelope of Backward-Wave Output Pulse at Increasing Angles of Tilt	57
Fig. 22	Variation of Peak Output Power with Angle of Tilt for Backward Wave (2410 Mc) Output of the Mod II Converter	58
Fig. 23	RF Waveform of Backward-Wave Output as Seen with Sampling Oscilloscope ( $f \sim 2400$ Mc)	59
Fig. 24	Voltage Envelope of Backward-Wave Output Pulse as Seen with Tektronix 535 Oscilloscope, Model K "Plug In"	59
Fig. 25	Variation of Pulse Energy with Angle of Tilt for Backward-Wave Output Pulse	60
Fig. 26	Schematic Diagram of Mod III Converter	62
Fig. 27	Oscillogram of Current Waveform in Discharge Using the Radial Wire Probe of Fig. 30 and the Sampling Oscilloscope (Hewlett-Packard 185B).	62
Fig. 28	Sketch of Current Sampling Probe	63
Fig. 29	Photograph of Resistive-Disc Electrode	64
Fig. 30	Photograph of Radial-Wire Resistive Electrode	65
Fig. 31	Electrode Designs	68
Fig. 32	Unbalanced, Shielded Hertz Oscillator	70
Fig. 33	Photograph of Mod IV Cavity Used	71
Fig. 34	Schematic Diagram of Proposed Mod IV Converter	72
Fig. 35	Output Spectrum of Mod IV Converter Cavity (Without pulseshaping filter)	74
Fig. 36	Breakdown Voltage vs. Gap Spacing	79
Fig. 37	RF Output vs. Gap Spacing	80
Fig. 38	RF Output vs. Gap Spacing for Different Materials	81
Fig. 39	RF Output vs. Firing Voltage	83

LIST OF ILLUSTRATIONS CONT'D

Illustration		Page
Fig. 40	RF Output vs. Firing Voltage for Different Materials	84
Fig. 41	RF Output as a Function of Firing Time	85



## I INTRODUCTION

The purpose of this program has been the investigation of the feasibility of using new techniques for the generation of very short pulses of microwave power with substantial energy per pulse. Typical operation desired was cited as being in C-band, with pulse lengths of 20 nanoseconds, 1000 joules per pulse. Pulse shape was not considered of primary importance, but should be essentially reproducible. Pulse repetition rate was also considered to be of secondary importance, but the principle employed should be capable of operation at repetition rates sufficient to make the device useful for radar application.

To give a feeling for the desired operation, we can observe that a square pulse 20 nsec. long with 1000 joules energy requires a power level of 50,000 megawatts.

The general principle that has been investigated in this program uses the sudden discharge of energy stored in a capacitance, and the coupling of the RF energy so generated through a suitable circuit.

It has been our purpose to investigate the possibility of the direct generation of RF power from dc stored energy. We have not considered harmonic generation to be within the scope of this work. Neither have we seriously considered the possibility of using accumulation techniques with a long pulse from a generator at normal power levels. By the latter, we mean the possibility of storing the energy of, say, a 10-megawatt, 100-microsecond pulse in a high-Q cavity (the decay constant must be at least of the order of magnitude of the input-pulse length), and then, by some suitable switching device, dumping all this energy into the load in 20 nanoseconds. It may be noted, however, that the key problem for an accumulator is the design of the switching

device. This problem is closely related to that of discharging a large amount of dc stored energy, with the added complication caused by the presence of high RF voltage during the hold-off period. Hence the work that we have done on the conversion of dc to RF power should have direct bearing on the design of a suitable accumulator.

In considering the requirements of the discharge, or switching device, we continue to believe that the only type showing prospects of being functional at the desired power levels is a spark gap. We include in this category devices such as the mercury-wetted reed relays which appear to function as a specialized type of spark gap. Thyratrons and other controlled discharge devices appear to act too slowly. Semiconductor devices such as the so-called "snap diodes" are limited to low voltages, at least at the present state of the art. Available high-vacuum devices using an electron beam do not appear practical for handling more than a few megawatts.

The circuit that couples the discharge energy to the output serves the purpose of controlling the pulse shape and the spectral distribution of power. In addition, it may influence the behavior of the spark by determining the impedance that is coupled to the discharge.

Many types of circuits are possible. In general, we have confined our attention to linear networks, although we did consider briefly the possibility of using a nonlinear capacitance. The latter investigation was dropped, since existing nonlinear materials which might be capable of operation at high voltage appear to have excessive loss at microwave frequencies. Rather than allowing ourselves to become involved in an extensive program of material development, we have concentrated on the use of linear transducers.

We have used four types of transducers, which we have designated as Mod I, Mod II, Mod III, and Mod IV. The Mod IV device was studied only briefly, near the end of the program. Each of the other main types has been further modified in the course of the work, as will be detailed later.

The Mod I transducer used, initially, the helix and 2-wire line design described in the original proposal. It was originally conceived as a microwave analog of the low-frequency structure of Hellar and Holter.<sup>1\*</sup> Emphasis was shifted to other types of circuits when it became apparent that it was not possible to make effective use of an extensively distributed capacity. The reasoning behind this conclusion will be discussed shortly. The experimental evidence confirming this conclusion for the specific system as originally conceived will be discussed in Sec. II-B-1.

The Mod II transducer used a tiltable meander line in rectangular waveguide. Its principal advantage for this program was that it was able to give detailed confirmation of theoretically predicted behavior. The transducer and the spark gap were sufficiently isolated from each other that the effect of each could be studied separately. This model, therefore, served as an excellent investigation tool, as will be described in Sec. II-B-2.

The Mod III system used a filter as transducer. A detailed description of the design and of the measurements taken on it will be given in Sec. II-B-3.

We had hoped that in the Mod III system, since the filter reflects power outside the pass band back onto the discharge, there would be a resultant improvement in efficiency. To a limited extent, an improvement does seem to occur. However, the situation is much more complicated than

---

\* References are listed at the end of the report.

it appeared at first glance. Specifically, any power reflected in such a way that it returns to the gap after completion of the initial switching transient sees an essentially fixed, although low, impedance. (We are neglecting possible nonlinear processes in the developed discharge.) Such power can only be either absorbed in the arc loss, or re-reflected without change in frequency. Hence it does little, if any, good to reflect power at unwanted frequencies unless the reflection occurs in the immediate neighborhood of the discharge.

The argument sketched above, which will be discussed in detail later, strongly suggests the desirability of incorporating the spark gap into the filter structure itself, so that the effect of the filter is felt within the time of the switching transient. It was this thought that led to the Mod IV design.

The development of an integral design, in which the spark gap serves as an important element of the filter, has its problems. Since the gap is both a time-varying element and one with nonlinear characteristics that may substantially affect overall performance, the design of an optimum filter using it poses design problems that have not yet been solved. Also, the precise behavior of a discharge, considered on a fractional-nanosecond time scale, is not known in detail, either from theory or experiment. The design must, therefore, be developed pragmatically from careful observations of the performance of complete systems.

The integral approach cited above and of which the Mod IV design is one embodiment, is, we believe, the one that will give the best results in the end. The other models, involving as they do a separation of the functions of the spark gap and the transducer, are useful for experimental purposes. But the final objective should be the development of an integral design.

## II TECHNICAL DISCUSSION

### A. General Principles

Before describing the detailed experimental work that has been done on the various models, we shall discuss some of the general principles that apply to discharge devices. The full significance of some of these factors has emerged only as a result of the detailed work to be described later.

#### 1. Switching Time

It is evident that one of the most significant parameters in the operation of the system is the switching time. Aside from the spark gap itself, the entire circuit is linear and time-independent. Hence the rest of the system can act only as a transducer, coupling out energy generated by the spark gap. The RF energy is generated by the spark gap primarily as a consequence of the variation of its impedance with time as the spark develops. This process can probably be approximated as a linear one, but one which is time varying. There is also the nonlinearity of the discharge even after it is well established. It seems likely, however, that most of the effects can be accounted for by the linear, time-dependent processes. If so, then the requirement that is of greatest importance is that the rate of variation of the gap impedance shall be fast enough to develop a significant signal at the desired frequency.

To consider this effect, we study the Fourier spectrum of the voltage across the gap. One of the significant parameters will be the microwave content of this voltage waveform.

If the waveform is an ideal step function, the voltage spectrum will be proportional to the reciprocal of the frequency. If the voltage pulse has a sharp front followed by an exponential decay to the quiescent voltage, so that the waveform is described by

$$V(t) = V_0 \quad t < 0$$

$$= V_0 (1 - e^{-\alpha t}) \quad t > 0$$

then, except for the dc component, the spectrum is given by

$$V(f) \propto 1/(j2\pi f + \alpha)$$

Hence the exponential decay of the tail of the waveform makes little difference unless the time constant of the decay is of the order of  $1/\omega$ , where  $\omega = 2\pi f$ ,  $f$  being the frequency of interest.

If, now, the switching time is finite, we get a further reduction. If, for example, the wave front is itself exponential, so that

$$V(t) = V_0 \quad t > 0$$

$$= V_0 \{e^{-\beta t} + 1 - e^{-\alpha t}\} \quad t > 0$$

where  $\beta$  is the time constant of the discharge and  $\alpha$  is that of the recovery, then, except for the dc component,

$$V(f) \propto \frac{1}{(j2\pi f + \alpha)(j2\pi f + \beta)}$$

Under normal conditions, the recovery will be slow, so that  $\alpha$  is small compared to  $2\pi f$ . If  $\beta$  also is small, indicating that the establishment of the discharge is also slow, then  $V(f) \propto 1/f^2$ . If  $\beta$  is large compared

to  $2\pi f$ , then  $F(f) \propto 1/f$  and the case approaches that of an ideal step wave. The transition between these two regimes is when  $\beta$  is of the same order of magnitude as  $2\pi f$ . That is, the response will be nearly as good as that of an instantaneous switch when the time constant of the discharge,  $1/\beta$ , is less than  $1/2\pi$  times a period of the RF signal.

This condition gives us a measure on the necessary speed of discharge. The time of switching (to the 90 percent point) is approximately two time constants if the waveform is truly exponential. Hence the maximum tolerable discharge time will be about  $1/3$  to  $1/4$  of an RF period.

The recovery time can be as long as we desire, at least without affecting this factor.

## 2. Hertz Effect

There is an additional effect that can theoretically be of considerable value in enhancing the effect of a spark gap. We have called it the Hertz effect.

Suppose the gap is built into a resonant circuit, so that the waveforms discussed previously are now the envelope of an oscillatory voltage. Specifically, suppose the waveform is given by

$$\begin{aligned} V(t) &= V_0 & t < 0 \\ &= V_0 \left\{ e^{j\omega_0 t} e^{-\alpha t} \right\} & t \geq 0 \end{aligned}$$

The Hertzian oscillation is now at  $\omega_0$  with decay constant  $\alpha$ . The Fourier spectrum is now

$$V(f) \propto \frac{1}{j(\omega - \omega_0) + \alpha}$$

In effect, the whole spectrum is shifted so that it centers at  $\omega = \omega_0$ . Since  $\alpha$ , the reciprocal time constant of the decay of the RF, is likely to be small, we can, in principle, obtain a large enhancement of the RF voltage at the desired frequency.

If  $\alpha = 0$ , so that the oscillation continues indefinitely, we obtain, in principle, infinite voltage at  $\omega = \omega_0$ . This implies no loss or coupling to an external load, so that this is not the condition that we want. Furthermore, we wish to limit the oscillations to the desired pulse length. The coupling to an external load will cause damping of the oscillation. Such damping, which in the simplest case, may be described by a nonzero value of  $\alpha$ , reduces  $V(f)$  at the resonant frequency to some finite value. However, the limited pulse length means that the output spectrum is broadened, so that we are now concerned with the behavior of the system over a range of frequencies. We must now ask what efficiency is theoretically obtainable under ideal conditions.

The Hertz effect is theoretically capable of giving us 100-percent efficiency. To see this, we consider a "gedanken" experiment with the system sketched in Fig. 1. We consider a cavity with a ball in the center. We assume that the cavity and the ball have no surface resistance. As a further simplification, we will assume that, after the discharge path has formed, the system will exhibit only a single resonance at  $f_0$ . We charge the ball up to a given voltage,  $V$ , and let it discharge to the cavity wall. We assume that the discharge is ideally lossless and instantaneous.

Initially the charge on the ball contained energy equal to  $\frac{1}{2}CV^2$ , where  $C$  is the capacity between the ball and the wall. If there is no



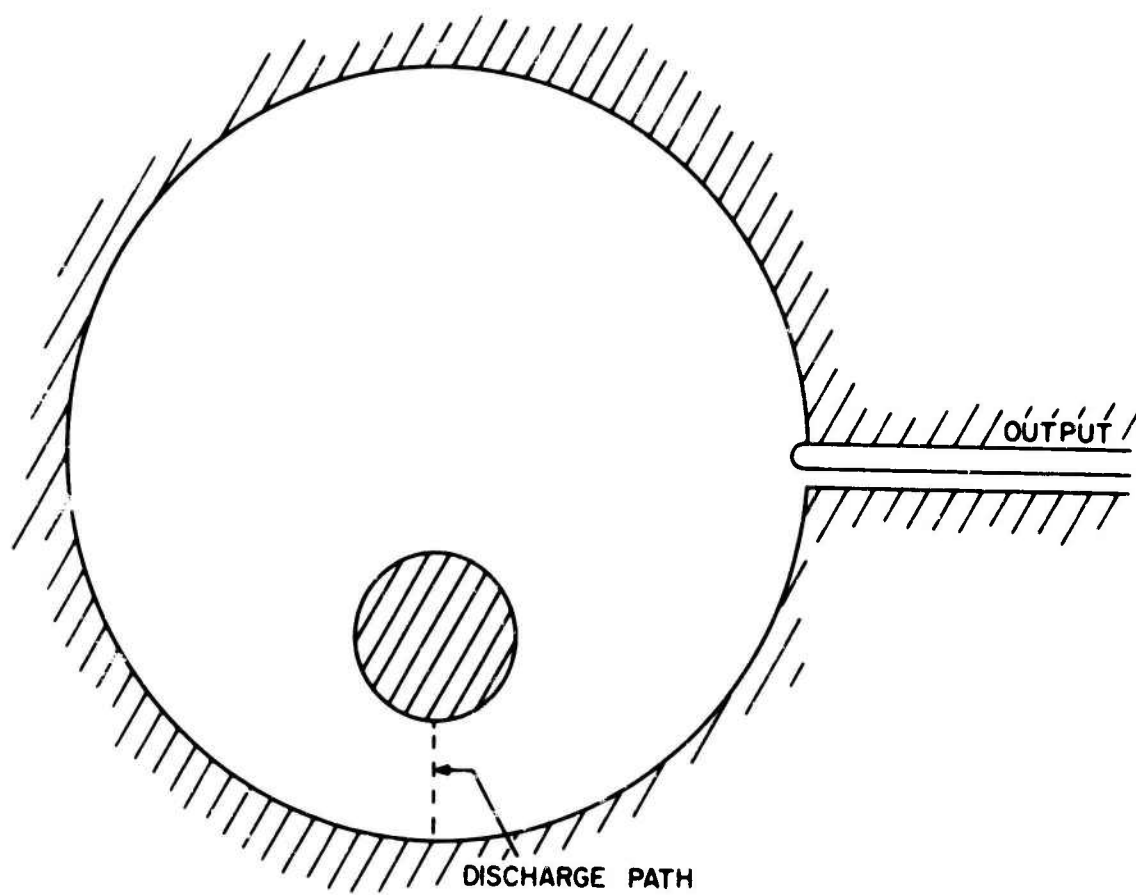


Fig. 1. Ideal Hertz Oscillator

output, this energy cannot be dissipated. Since the cavity is assumed to have only the single resonance, the energy must all go into that resonance at  $f_0$ .

If, now, we introduce an infinitesimal coupling loop, we will slowly drain all the energy in the cavity. Hence we obtain all of the initial energy at frequency  $f_0$ .

As the coupling is strengthened, we obtain a band of frequencies. The pulse starts abruptly and oscillates at  $f_0$  with an amplitude that decays exponentially as the energy in the cavity is depleted. Hence the spectrum is, as before, proportional to  $1/(j2\pi f_0 + \alpha)$  where  $\alpha$  is the decay constant. The spread of energy indicated by this function is due to the lowering of the effective  $Q$  of the cavity by the output loading. Nevertheless, all the stored energy must eventually be delivered to the load, since there is no other place for it to go. Hence, the efficiency of the system must remain 100 percent.

We may ask, now, what happens in the unloaded system if the switching time is made finite. The answer depends on just how it is limited. If the discharge path is lossy, it may damp out the resonance before it ever gets started. Thus we can lose energy rapidly.

On the other hand, we can slow the discharge without loss by making it purely inductive, perhaps with the inductive reactance slowly decreasing to zero. To see what happens, we consider again the case where the cavity is not coupled to the output. If the discharge were a fixed inductance, it would modify the resonance of the system. There must evidently always be a resonance such that the discharge can drive it. For the energy

has to go somewhere, and there is no other place for it to go. If, now, the inductance of the discharge decreases with time, the resonant frequency will increase. Since the  $Q$  of the cavity is infinite, the frequency of the stored energy must change with the resonant frequency. The effect is that the cavity is initially excited at the lower frequency. The energy in the resonance is then walked up to  $f_0$  by the parametric effect of the varying inductance. If now, we introduce an infinitesimal coupling to the output, we must again obtain 100-percent efficiency.

The argument given immediately raises the question of the significance of loss during and after the establishment of the discharge. The argument assumed that the discharge was lossless, and exhibited at most a time-varying inductance. A practical discharge, however, must exhibit loss even in its steady state condition, and probably has substantial additional loss during its time of formation.

The steady-state loss of the discharge will simply contribute an additional damping mechanism. It may be described by the effective unloaded  $Q$  of the cavity with an established discharge.

Additional loss during the discharge transient is a much more difficult matter. This loss is describable as a time-dependent component whose rate of variation is comparable to the rate of oscillation caused by the Hertz effect.

A similar phenomenon has long been recognized in low frequency, lumped-constant, ringing circuits--e.g., in the fly-back circuit of television. It is known that it is very important that the switching be very rapid--a small fraction of a cycle--to avoid excessive loss.

The mathematical analysis of the effect of a transient loss or reactance is difficult. Even with the simplest possible description of the spark impedance, the differential equation that describes the system is a complex one. For example, if we assume the spark impedance is a pure resistance that varies as  $k/t$ , the equation appears to be a transformed Bessel equation of fractional order. We have not investigated what the equation might look like with more complex time variations, or with time varying reactive components. It probably would be worthwhile to investigate the behavior of such systems by calculations aided by a computer.

Regardless of the details of the behavior, it is evident that it is of vital importance that the switching time be short. We suspect that, under the present circumstances, the behavior of the system is even more sensitive to switching time than was calculated in the previous section. We might guess that it is necessary that the switching time be held to perhaps 0.1 or 0.2 of an RF cycle if the resultant RF loss is to be held to a reasonable value.

### 3. Multiple Spark Gaps

We have repeatedly considered the possibility of using multiple spark gaps to increase the power. One can consider the possibility of using several gaps in parallel, or in series, or in some combination of parallel and series connection.

#### a. Parallel Operation

By parallel operation, we mean two or several gaps, each switching its own capacitance, and each contributing its share to the total RF output.

It is not difficult to think of circuits that could make effective use of parallel gaps. Most simply, perhaps, we can consider a section of waveguide with a number of resonant antennas in it, each charged to the selected voltage, and each switched by its own spark gap. A somewhat simplified circuit of this type is sketched in Fig. 2(a). The diagram shows a waveguide with a wire down the center to carry the high voltage. The center conductors of the stubs, which are made to be resonant after discharge of the spark gaps, are connected to this line through isolating impedances. The coupling of each stub to the waveguide is adjusted to give the desired pulse length.

If we could arrange matters so that the gaps would fire in predetermined sequence with a time delay corresponding to their electrical separation, the elements would act cooperatively to produce the total output.

The difficulty, of course, is to obtain the necessary synchronization. It is not difficult to see that the elements must be synchronized within a fraction of a cycle of RF.

Consider, for example, two gaps in the arrangement of Fig. 2(a). Suppose that they do fire within, say, a nanosecond of the correct time, so that their separate contributions at least occur within the 20-nanosecond pulse. Tight as this requirement on synchronization is, we will suppose it has been achieved in some way. As we will now show, even this requirement is not sufficiently tight.

Suppose the two gaps are separated by an effective half wavelength. If, now, the second gap fires a half cycle after the first, or an odd multiple of a half cycle, the signals will reinforce each other. This is the desired mode of operation.

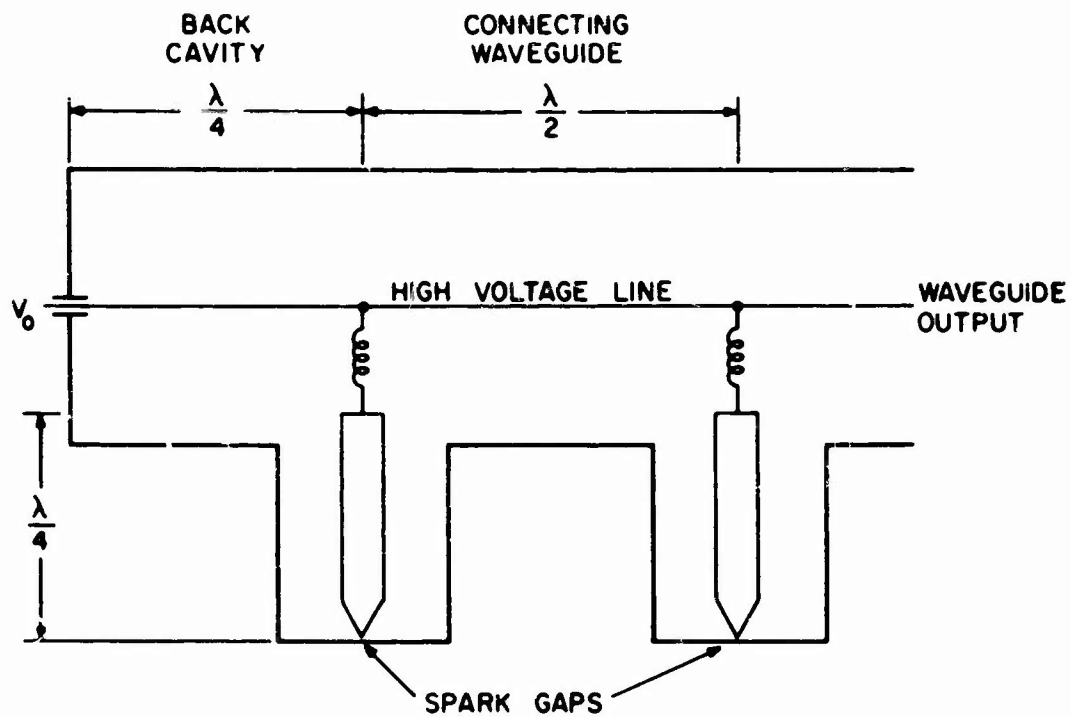


Fig. 2(a) Multiple Generators in Parallel without Synchronization

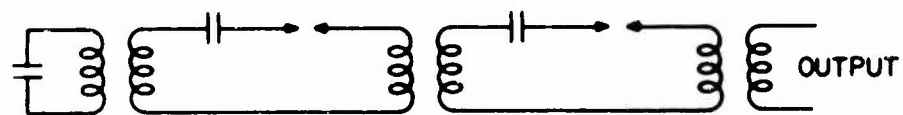


Fig. 2(b) Equivalent Circuit

If, however, they fire at the same time, or at an integral multiple of a period, then the signal from the second gap will precisely cancel the signal from the first. The output at the operating frequency will be zero. Neglecting loss, the stored energy must go somewhere. We must then ask what happens to it? The answer lies in the equivalent circuit of Fig. 2(b). The separate resonant elements, after the first, which represents the back cavity, represent the resonant stubs. The connecting sections of waveguide can be ignored as long as they are a half wavelength long. We have, then, a set of three coupled resonant circuits. This system has three distinct resonant frequencies, since the degeneracy of the coupled circuits is split by the coupling. Only one of these frequencies is the design frequency.

If the circuit is excited in such a way that there can be no output at the design frequency, then the released energy must excite one or both of the other resonances. More generally, if the discharge of the separate elements is not so synchronized as to confine the excitation to the design frequency, the system will distribute its energy randomly among the various other possible resonances of the system.

It is, therefore, essential in parallel operation that all gaps be synchronized with time delays of .1 or .2 nanoseconds at S band within a small fraction of a period.

The circuit of Fig. 2(a) includes no provision for synchronization except through the RF coupling itself. One can consider various possible means of control. The use of an auxiliary control electrode in each gap is one. Another possibility is the design of a multiple gap system in which each

gap is optically coupled to the others. It is known that the ultraviolet light generated in one spark gap does tend to induce breakdown of a similar gap. Coupling through the RF field is still another possibility.

If it is possible to synchronize parallel gaps sufficiently accurately, then the separate outputs of each gap will add constructively, and will permit obtaining high power without increase of operating voltage.

We have felt, however, that the required degree of synchronization would be very difficult to obtain. We have also considered it necessary to learn first how we can make the most effective use of a single gap. Given a sufficient understanding of the capabilities of a single gap, and knowledge of how these capabilities can be realized, it will then be appropriate to consider whether it will be better to accept the requirement of multimegavolt operation, or whether we should in fact put major effort on learning, if possible, how parallel spark gaps can be synchronized. We have, therefore, deferred study of the synchronization problem, and have concentrated on studying the behavior and design of single gap configurations.

b. Series Operation

By the series connection of multiple spark gaps, we refer to the kind of system that is sketched in Fig. 3.

The purpose of this arrangement is to permit the application of a higher voltage without increase of effective gap width. Since the power stored in the system is equal to  $\frac{1}{2}CV^2$ , doubling the voltage multiplies the output power by four, other things being equal.



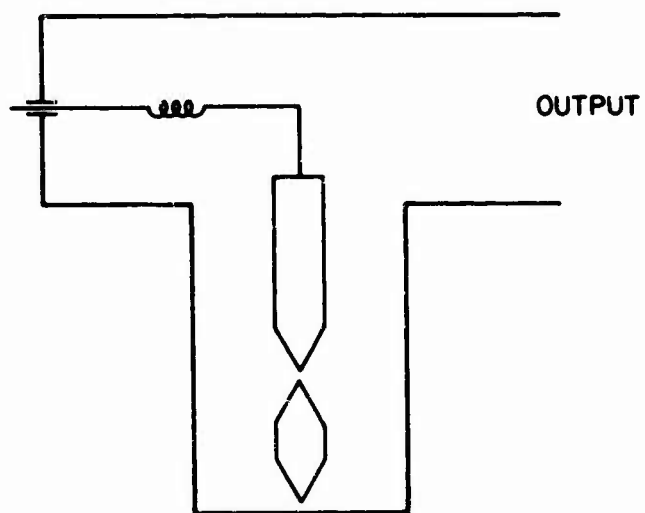


Fig. 3 Series Connection of Two Gaps

The question of synchronization does not arise in this configuration, at least to the first order. The energy stored in the stub is not released until both gaps have fired. Hence the effective gap is the last one, which acts essentially by itself. The firing of the first gap has as its principal effect the imposition of a high over-voltage on the second.

We do not regard this as a pulse-sharpening technique. For two gaps in series to function as a pulse sharpener, it is necessary that the gaps be separated by a sufficient distance so that the second gap, which is arranged to be the shorter one, has voltage on it only after the first gap has completely fired. In the arrangement considered here, the two gaps are so close together that there is only an inappreciable time delay between them. The voltage, furthermore, is impressed across both gaps simultaneously. Indeed, it is probably desirable to insert a leakage path to ensure proper division of the voltage drop between the two gaps.

The purpose of this type of arrangement is solely to allow an increase of voltage with no increase of discharge time.

Several comments regarding this scheme are pertinent. Firstly, the loss of the discharge is, of course, doubled by putting two discharges in series if no other adjustment is made. It is possible that the additional loss can be partly compensated by adjustment of the gap length with only minor sacrifice of hold-off voltage. However, it is likely that this factor will limit the number of gaps that can be used effectively.

Secondly, we may observe that the effect discussed above refers primarily to the steady-state loss, and so may be discussed in terms of

the unloaded Q of the system with the developed discharge. In discussing the Hertz effect, we also noted that there is undoubtedly an additional transient loss during the period of formation of the discharge. We suggested that this might be a very important factor in limiting the effectiveness of the Hertz effect.

If, now, the two gaps do not fire exactly synchronously, the transient loss of the first gap may have disappeared before the second gap fires. If so, then the effective transient loss of the combination will be only that of the second gap. There will be no increase of the transient loss due to the multiple gap arrangement.

If this argument proves valid, it may be an important benefit of using multiple gaps in series.

We may also observe that there are second-order effects if the gaps do not fire simultaneously. If, in Fig. 3, the lower gap fires first, the energy stored in the intermediate section is discharged first. There will, then, be a readjustment of the charge on the upper section which will slightly reduce the energy stored there. Both these effects will generate higher frequency signals if the discharge is sufficiently rapid. or loss otherwise. The frequency, however, will be much higher - well out of the operating band of the system. Hence, in either case, the effect is primarily one of loss of efficiency and power. If the principal part of the total capacity is in the upper section of the stub, the loss will be small

Initial work with double spark gaps has confirmed the possibility of using the principle to obtain higher operating voltage and output power. However, applicability of the principle depends on the design of the

system--particularly on the extent to which the system is limited by the steady state loss of the discharge. The method is to be regarded, therefore, as one whose applicability must be separately determined in each design.

#### 4. Electrode Shape

The experimental evidence tends to indicate that the best performance is obtained with at least one electrode being initially pointed. This is somewhat surprising since it has been generally considered that the fastest discharge for a given holdoff voltage is obtained with nearly flat electrodes.

In the statement given above, we have used the phrase "initially pointed." With operation, the point erodes, losing its sharpness in the first few seconds. Since the gap spacings we have used have been small--generally only a few thousandths of an inch--not much erosion is needed before the actual discharge comes to act as if the surfaces were nearly flat. It can be argued, therefore, that we are obtaining the benefits of nearly flat electrodes, and that the improvement we observe is due to the effective minimization of other, potentially adverse side effects.

One of the significant side effects of flat electrodes is the relatively large capacity directly associated with the gap. The field lines that cross the gap along or parallel to the discharge path have only weak coupling to the RF field that we seek to generate. Hence, the fraction of the stored energy represented by these lines of force is less easily used effectively. We conclude, then, that it is desirable to minimize the gap capacity as much as possible without sacrifice of other parameters. A pointed electrode does help to reduce the gap capacity. It may be this reduction that is the primary cause of the effect we have observed.

We should also observe that there is a significant difference in the criteria being used to judge performance. Workers who have studied the performance of spark gaps in isolation have usually measured either switching time for a given holdoff voltage, or voltage holdoff for a given switching time. In either case, the gap width has been adjusted to hold constant the indicated parameter.

In our work, we have generally applied the voltage through a high impedance circuit--typically 2 megohms. We have adjusted the gap width to obtain maximum RF output. The latter is a function of both the actual firing voltage and the switching time. The actual firing voltage, due to the isolating impedance, is lower than the supply voltage, and is also a function of the gap width. This is, then, a very different criterion than the usual one of switching time at constant holdoff or holdoff at constant switching time.

The observed results, and the discussion given here, emphasize again the necessity of studying the entire system as a unit. In the work done so far, we have found it desirable to point one of the electrodes to about a 90-degree cone angle. However, even this result should be considered as contingent on the specific system being used. With a different system, or with the gap operating in a different environment, it would not be too surprising to find a somewhat different optimum condition.

##### 5. Discharge Atmosphere

We must also ask what should be the atmosphere of the discharge? What should be its pressure and composition?

Regarding pressure, there seems to be no doubt of the desirability of using as high a pressure as is mechanically feasible. High pressure should permit us to achieve high voltage without sacrifice of switching time.

One might, conceivably, consider operation on the low-pressure side of the Paschen curve to obtain high voltage operation. It appears very likely, however, that this type of operation would be quite poor. The rise of voltage with decreasing pressure at sufficiently low pressures is due to the capture of free ions and electrons by the electrodes. If the length of the discharge path is less than the mean free path length of an ion or electron, the collision probability is decreased, and breakdown is inhibited. At sufficiently low pressure, the discharge must be entirely maintained by the emission of ions or electrons from the electrodes themselves, rather than by collision ionization of the gas molecules.

A discharge sustained by emission from the electrodes would probably be a slow one since, according to the usual theory, it depends on the movement of relatively heavy ions. Further, we might expect it to be a high-impedance discharge, thus accentuating the loss. It is for this reason that we have believed the high pressure discharge to be the more suitable type for the present device.

On the question of the composition of the gas, the argument is not as clear. To obtain maximum hold-off voltage in a constant geometry and pressure, we need a gas with as high an ionization potential as possible. We would also like to have present a gas with good attaching properties to reduce the probability that an isolated event will trigger the discharge.

The problem is not this simple, however. We are willing to adjust the gap width for maximum output. It may be that we will actually be able to use a higher voltage with a gas that is more easily ionized if it permits us to use a wider gap. This will be true if the gas, because of its easier ionization, reaches full ionization more rapidly once the process is started.

For the same reason, the presence of an attaching gas may be highly detrimental in terms either of switching time or of loss.

Part of the difficulty here is the extremely short time that is involved. We seek switching times of the order of 0.1 to 0.2 nanosecond. This is certainly far shorter than is required to reach an equilibrium plasma. It is not fully apparent, in fact, what is the mechanism that permits us even to approach this fast a process.

The determination of the optimum gas composition is a question that has been left for future work. The immediate requirement was to obtain basic understanding of the electrical and RF processes involved. Since it seemed unlikely that the gas composition would have any very drastic effect on the operation, we have deliberately deferred this question.

#### 6. Distributed Storage

At the start of the program, we had hoped to be able to make effective use of large energy storage at reasonable voltage by using a capacitance that was distributed over an extensive region. This was the initial concept of the Mod I design.

We rather rapidly came to realize that this concept could not be implemented and that energy, to be effectively utilizable, had to be stored electrically close to the discharge. By "close" we mean within a fraction of a wavelength at the desired RF.

The reason for this conclusion is that the key factor that is involved in the generation of the RF is the switching interval. Before and after the switching interval, the system is linear, and so generates no RF. Consequently, the RF energy that is formed must be determined by what happens to the discharge during the switching interval.

By "switching interval" we do not necessarily mean the same thing as "switching time." The latter is a measure of the time it takes for the impedance of the gap to change from its high initial value to a low one. By the former we mean the time during which the impedance of the gap is varying significantly. It may happen, for example, that the initial effect is the decay of the impedance from its initial value to a small reactive one, followed by a period in which the reactive impedance becomes resistive. This latter shift may also have a significant influence on the generation of RF energy. Hence the switching interval may be appreciably longer than the switching time. It is hard to imagine, however, that it can be longer than, say, an RF period and still have a significant influence.

We discussed some of the implications of the behavior of the gap during the switching interval in the section on the Hertz effect. There we considered the behavior of the ideal circuit of Fig. 1 with a discharge that was lossless but included a time-varying inductance.

The general conclusion we have reached is that any energy stored more than a fraction of a wavelength away from the gap cannot contribute to the RF energy.

As an illustration and example of this principle, consider the circuit of Fig. 4 as a simplified Hertz oscillator. This is a section of coaxial line with a spark gap a distance  $L$  from an open-circuited end. The other end feeds through a length of line to a bandpass filter. We may initially suppose that the filter absorbs energy in all frequencies outside its passband. We neglect loss elsewhere in the circuit, and assume that the discharge is formed instantaneously without loss. We charge the length  $L$  to a given voltage,  $V$ , and then let the gap discharge. After discharge,



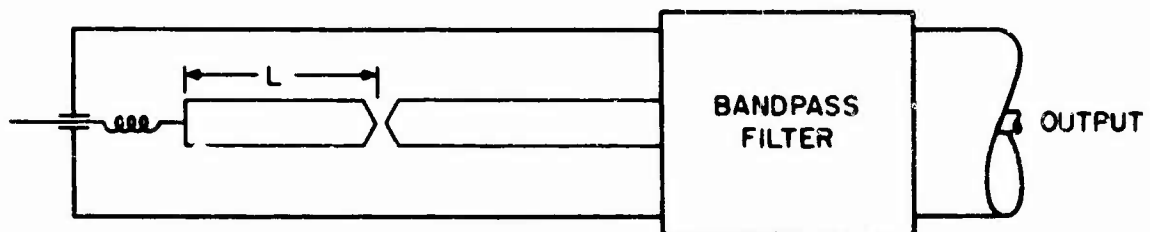


Fig. 4 Simplified Circuit of Coaxial Generator

we obtain a square pulse of voltage of height  $\frac{1}{2}V$  and length  $2L$  that propagates down the line to the filter. If  $L$  is large, the output from the filter will be in the form of two RF pulses whose length depends on the width of the pass band, separated by the distance  $2L$ , and of opposite phase. These, in effect, are generated by the leading and trailing edges of the square pulse into the filter. Increasing the length  $L$  only acts to separate the two output pulses. It does not affect the power in either pulse. It is evident, in this case, that the energy of the RF output is the same, independent of the additional stored energy provided by increasing  $L$ .

If the filter is reflective rather than absorptive outside its passband, the result is the same except that the reflected energy must now bounce back and forth indefinitely between the open circuit and the filter.

If we shorten  $L$ , nothing significant happens until the two output pulses start overlapping. When  $L$  reaches a quarter wavelength of the center frequency of the filter, the two pulses reinforce each other. This is the Hertz effect noted above when the discharging circuit is resonant at the frequency of interest. In this case, the effect is limited since the length  $L$  is very heavily coupled to the main transmission line, with the bandwidth being limited by the filter some distance down the line. Hence the Hertz oscillator has a very low loaded  $Q$ . Yet even in this situation we note that the Hertz effect has some influence.

If  $L$  is further decreased, the two pulses start destructively interfering, with reduction of the output power.

We conclude that it is not enough that the requisite energy be stored in the circuit prior to discharge. It is also necessary that it be

stored in such a way that it is affected by the discharge within the appropriate switching interval. It must, in other words, be stored within a fraction of a wavelength of the physical location of the discharge. This conclusion has been verified experimentally in the Mod I system. It has also been observed indirectly in the other systems where we have seen that the maximum RF output under optimum adjustment is relatively independent of the external circuitry.

## B. HISTORICAL NOTES AND SURVEY

### 1. Discharge Oscillators

The principle of obtaining RF energy from a circuit by a transient discharge has a history going back to 1888.<sup>2</sup> The operation that has been of practical interest, then and now, has used the discharge of capacitively stored energy through a spark gap. Landmarks of achievement include the generation of wavelengths as short as 0.5 cm (by Bose<sup>2</sup> in 1897) and of initial peak powers as high as several hundreds of megawatts (at 24 Mc, by Dolphin and Wickersham<sup>3</sup> in 1964).

It is of value here to re-examine briefly the classical microwave generators in the light of present-day understanding. The meter wavelength generators of Hertz and Marconi can be reduced to the essentials shown in Fig. 5(a). The unbalanced versions--Figs. 5(b,c)--were not reported on, but they might be better suited for re-examination in a modern laboratory. The essentials of the centimeter-wave generators of Bose, Lodge, et al.<sup>2</sup> can be represented as in Fig. 6.

In Fig. 5, if the spark gap fires as a simple step function, a continuum of frequencies would be contained in the spark current. However,

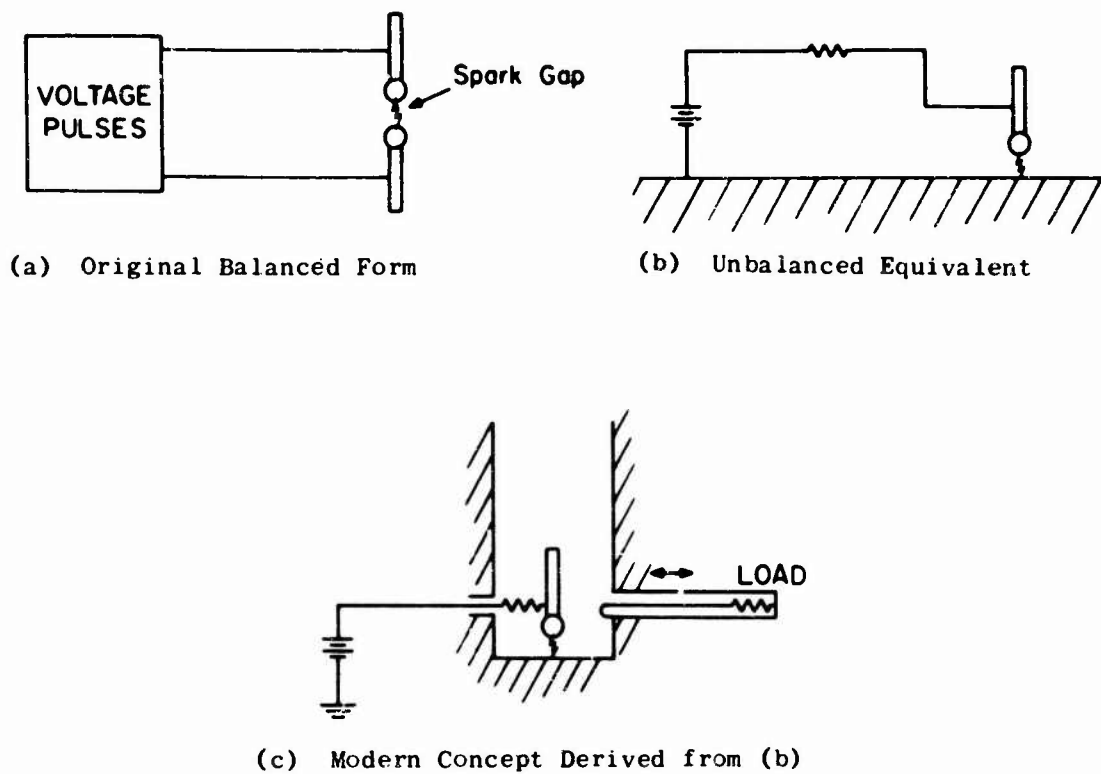


Fig. 5 Essentials of Classical Meter-Wave Generators

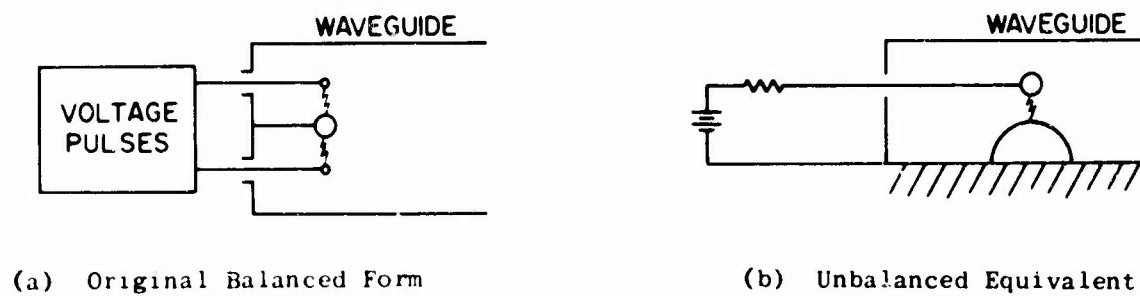


Fig. 6 Essentials of Classical Centimeter-Wave Generators

the signals generated were detected only after propagation through space, so that energy would be observed principally at the lowest frequency at which the dipole radiation resistance has a peak value. Thus, one could not, in a simple, qualitative test, determine whether the spectrum of the spark current had a peak at  $\omega = 0$  with the dipole-transmission medium-receiver system acting merely as a tuned filter or whether, as is commonly assumed, a substantial portion of the spark current oscillates at the dipole resonance frequency ( $\omega_0$ ) so that the spectrum develops a peak at  $\omega_0$ . If the resistive and radiation loading was high, so that the generator exhibited a low value of loaded  $Q$ , as may well have been the case, it may be doubted if oscillation of the current played a significant role. As a possible confirmation of this, Hart<sup>4</sup> studied a system employing wideband coupling and detection equipment, and failed to find any peaks of the output near the expected resonance.

The shielded half-dipole of Fig. 5(c) is a logical development from the open dipole of Fig. 5(a). The shield permits direct control of the coupling factor, allowing the  $Q$  of the circuit to be fixed, as desired, up to its unloaded figure. It would be of considerable interest to study this system scaled to a frequency that is sufficiently low to permit detailed study of the processes involved.

In Fig. 6, which is schematically the circuit studied by Bose, Lodge, et al., we suspect, again, that the loaded  $Q$  of the discharge circuit was sufficiently low so that little, if any, current oscillation occurred. The voltage spectrum of the radiation from the discharge itself would then be proportional to  $1/f$ , up to the frequency at which the discharge time becomes

significant. The coupling circuit in this case consists of a waveguide, so that its transmission characteristic exhibits a low-frequency cutoff. The detected output, neglecting the effect of the coupling circuit back on the spark-gap itself, is then the product of the radiation spectrum of the gap and the transmission characteristic of the waveguide. The product of these factors will peak at a frequency ( $\omega_1$ ) slightly above the cutoff frequency of the waveguide. This type of behavior has been described by Saxton and Schmitt,<sup>5</sup> and confirmed during this program by observation on the Mod I and Mod II systems.

Whether or not the classical workers<sup>2,6,7</sup> relied exclusively on the waveguide effect is not known. The metal spheres they used were thought to establish a definite frequency ( $\omega_0$ ) of spark-current oscillation, but it is not known whether the loaded Q was sufficiently high for a strong current oscillation to have developed or whether  $\omega_0$  was sufficiently close to  $\omega_1$  for such an oscillation to have affected the output. The output would also have been affected by too slow a rise time of the spark current, predictable from the reduction in spectral content of the spark current at the higher frequencies, whether peaked there or not.

Although the Dolphin and Wickersham<sup>3</sup> device is designed for low frequency operation, it has features that are pertinent to a microwave spark-generator survey. In particular, it makes successful use of multiple spark gaps, in a large ring containing several dozen each of capacitors and spark gaps in series. As seen in Fig. 7, the spark gaps are charged in parallel, but when discharge occurs, they are in series and have a common current.

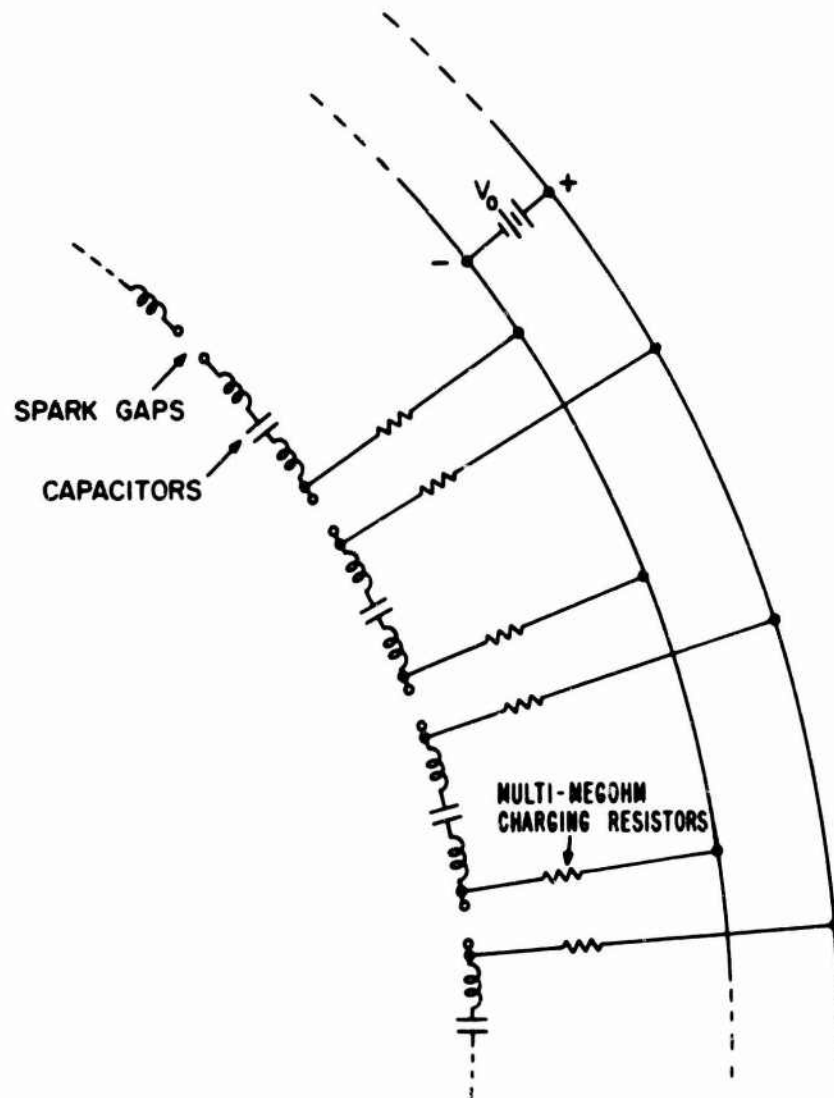


Fig. 7 Spark-Gap Ring Transmitter of Dolphin and Wickersham

The series connection of the spark gaps assures that they will fire in at least approximate synchronism. In addition, there are holes through the electrodes to permit ultraviolet light from one gap to reach neighboring gaps, thus aiding synchronization.

It is questionable if the effective discharge time of the whole circuit, as presently designed, is very short. At the operating frequency of 24 Mc, a rapid discharge is not necessary, but this would become a critical factor in any attempt to scale the device to microwave frequencies.

The capacitors in Fig. 7 can be no larger than the value required to tune the ring to the desired frequency. Thus the energy available for conversion can be no greater than that stored in these relatively small capacitors prior to discharge. No energy can be added from the power supply as the feed lines contain large isolating resistances (and inductance) to prevent loading of the ring.

A closely analogous situation prevails in the high frequency generators of Figs. 5 and 6. The size of the wires bringing in charging current was chosen so as not to load the dipoles. The wires thus have too large an inductance to allow appreciable energy to flow from the power supply to the dipole during the discharge. Hence, the energy available for conversion in this type of device is limited to what can be stored on the spheres or dipole cylinders. This limitation appears fundamental and applies to any conceivable spark converter, classical or modern.

## 2. Coupling Circuits

One of the sources that led us to the initial consideration of spark gap generators was the work of Hellar and Holter.<sup>1</sup> Their circuit is shown in Fig. 8. It was designed to operate at 100 kc, and to deliver pulses of 10-cycle duration.



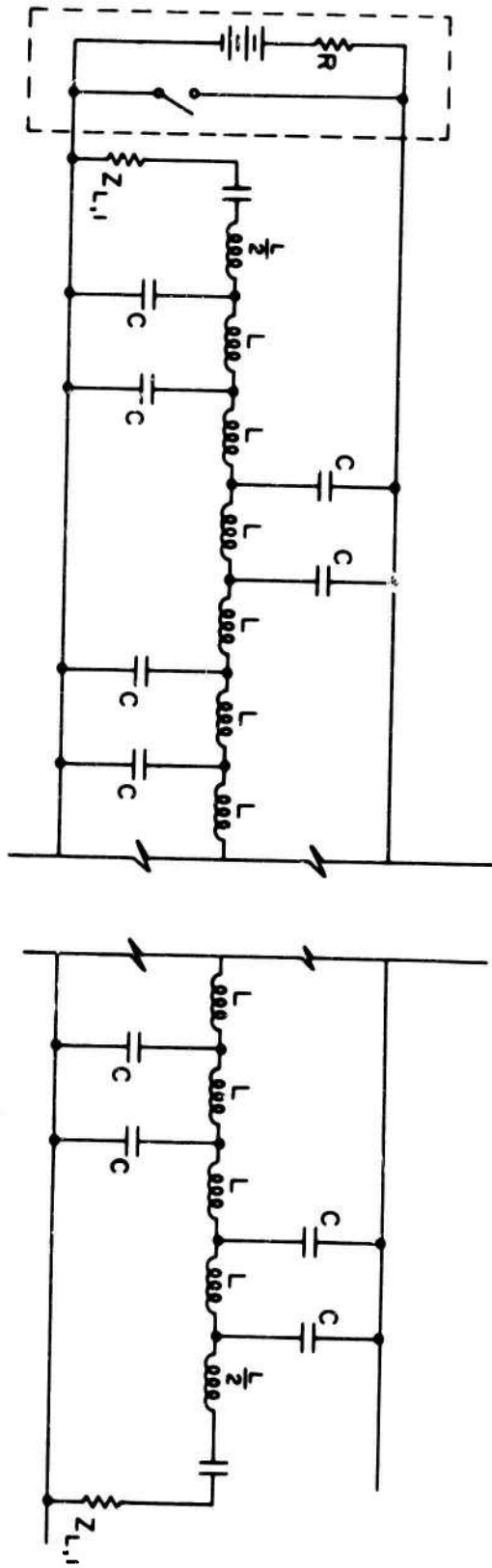


Fig. 8 Circuit of Helar and Holter

The operation of the circuit may be described as follows: Initially, the outer lines are charged to the battery voltage through the isolating resistor,  $R$ . The center line is at an equipotential, so that each capacitor has the appropriate voltage drop across it. When the switch is closed, the outer lines are brought abruptly to a common voltage. The charges on the capacities force the center line to exhibit an approximately sinusoidal voltage variation along it. When the outer lines are shorted through the switch, the whole system becomes a lumped-circuit approximation to a transmission line. Hence the sinusoidal variation of voltage along the center line resolves into two traveling waves which travel off the line into the two load resistances,  $Z_L$ .

The original Mod I circuit was intended as a microwave analog of this circuit. It was deduced that the finite speed of propagation of the discharge along the two-wire transmission line formed by the outer lines of Fig. 8 would not be harmful. Its effect would be to introduce a Doppler shift in the frequencies on the two waves. Instead of being at the same frequency as indicated by Hellar and Holter,<sup>1</sup> the frequency of the forward wave into  $Z_{L1}$  in Fig. 8 would be increased, and that of the backward wave into  $Z_{L2}$  would be decreased. This Doppler shift appeared to be advantageous in that it would permit the use of a larger structure for a given forward-wave output frequency.

Another way of viewing the circuit of Fig. 8 has emerged in the course of our work. We can observe that the elements in the dotted rectangle on the left are the only ones that are not linear, homogeneous, passive, and constant. Hence if we neglect the loading of the switch by the circuit, we can view the components in the dotted rectangle as a generator that delivers

a broad-spectrum output in the form of a step wave of voltage. The circuit, then, acts as a selective filter to develop the observed output pulse.

It was this point of view that led to the later versions of Mod I and the circuit of Mod II.

### 3. Spark Gaps

The literature on the design and measurement of spark gaps is very extensive, but only a small part of it appears to be significant for microwave type of operation. A short annotated bibliography of those references that appear to be pertinent is given as Appendix A.

## C. EXPERIMENTS

### 1. Mod I

Our first experiments in microwave energy conversion were performed at L-band. Two coupled transmission lines, 12 feet long, were built of copper and brass. The first transmission line was a parallel-wire line (1/4-inch rods spaced 3.75 inches on centers) on which a voltage step would propagate at the speed of light. The second, or slow-wave, transmission line was a helix (3/16-inch wire at 8.5 turns per foot on a 4.5-inch diameter) surrounding the two-wire line [Fig. 9(a)]. Coupling between the two lines occurs near the frequency (nominally 830 Mc) for which the developed length of one turn of the helix is one wavelength. At this frequency, the helix would radiate strongly into the room. Hence, a 9-inch-diameter cylindrical shield was added to confine the radiation. This shield also facilitated providing simple and fairly well-matched transitions from coaxial connectors to the ends of the helix. To be precise, the two lines within the shield should couple maximally at two frequencies, approximately 10 percent above

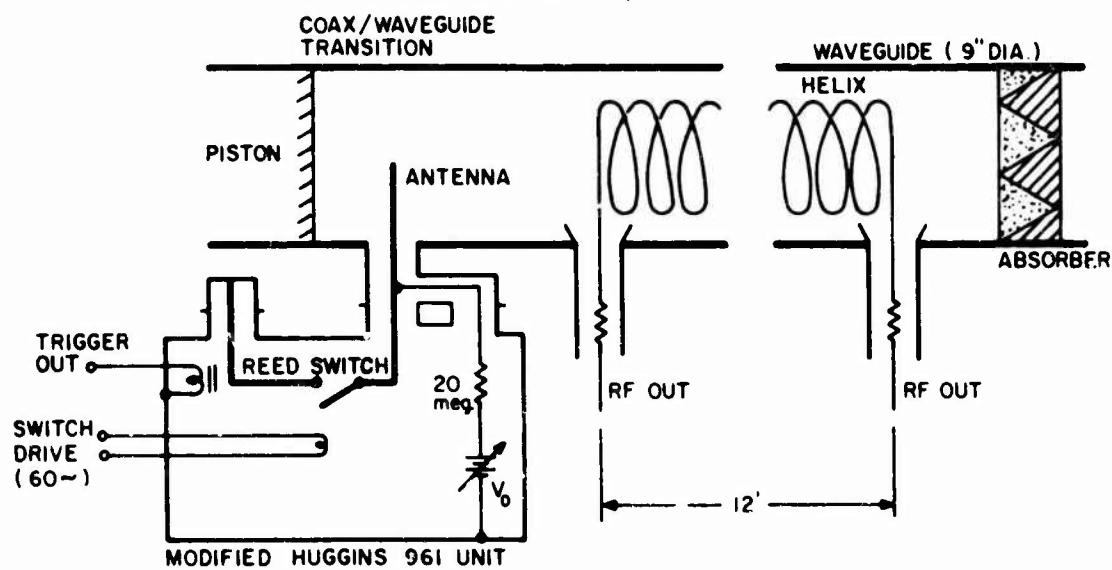
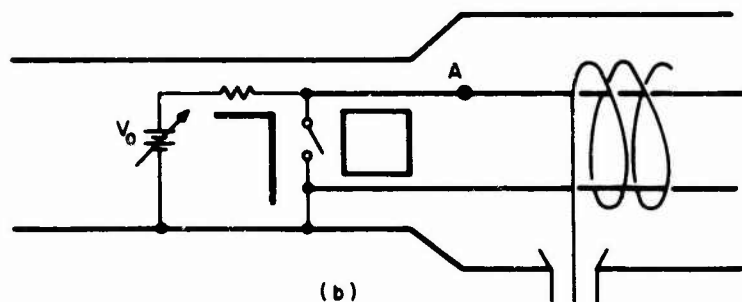
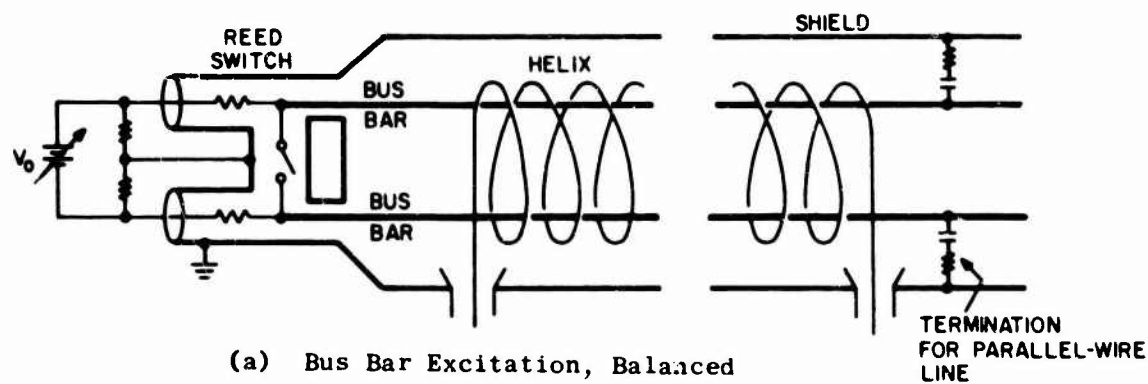


Fig. 9 Schematic Representation of Mod I Converter

and below the nominal frequency, according to the relative directions of propagation. The plastic pieces used to support the metal conductors would modify the predicted frequencies, as would the perturbation of the mode of one transmission line by the conductors of the other. Additional electrical and construction details are shown in the schematic drawing.

To launch a voltage step onto the two-wire line, a voltage source is applied through charging resistors, following which is a fast-acting switch, to be described later. The RF behavior of the device was found to be independent of whether the voltage source and switch were connected in balanced [Fig. 9(a)] or unbalanced [Fig. 9(b)] fashion.

It was at first believed that the Mod I apparatus would represent a valid analog of the Hellar-Holter device, with the several capacitances formed between the helix wire and the longitudinal rods being the capacitances to be discharged through the switch. Later, it was realized that, at microwave frequencies, a workable analog of the Hellar-Holter device would probably require a switch to be associated with each capacitance, with all the switches appropriately synchronized. Instead, the simplest interpretation of the operation of the apparatus of Fig. 9 is that the transmission lines constitute merely a passive, frequency-sensitive, directional coupler to extract energy from the spectrum of the voltage step in the desired frequency band and to shape the pulse envelope. We may note that it is possible to view the original Hellar-Holter device in the same way--i.e., as a frequency-sensitive directional coupler extracting energy from the spectrum of a step function. (The spectrum referred to would, of course, be modified if appreciable Hertz-type oscillations are superposed on the switch current.)

Confirmation that the circuit of Fig. 1(a) acts merely as a filter/coupler and that, in particular, the sole effect of the two-wire line is to propagate a linearly polarized fast-wave, was obtained in part by accident. While observing the RF output of the system, a gap was allowed to occur at A in the upper rod in Fig. 9(b). Instead of becoming zero, the RF output power increased slightly. The interpretation made was that the shield, acting as a waveguide excited by the antenna formed by the remaining bit of rod at the ungrounded side of the switch, had taken over the function of propagating the linearly polarized fast wave. This phenomenon was quickly taken advantage of, especially as removal of the longitudinal rods had no further effect. From then on, we worked with the set-up of Fig. 9(c), noting that the left-hand portion acts as an "exciter" and the right-hand portion as an "extractor," with a simple waveguide between. When the switch closes, the static voltage on the antenna drops quickly to zero, launching energy at all frequencies. Only energy at frequencies above the cutoff of the waveguide is propagated to the right. From this energy, the helix extracts two narrow bands by forward- and backward-wave interaction. Energy at frequencies above waveguide cutoff, but outside the bands extracted by the helix, is absorbed at the far end of the waveguide. High-voltages and high-power levels associated with frequencies below the waveguide cutoff are confined to the exciter end of the device, avoiding heat and insulation problems in the extractor portion.

The major defect, for experimental purposes, of the device of Fig. 9(c) is that the coupling coefficient between the helix waves and the fast wave is not optimized. For example, the length of the coupling section

determines the length of the pulse which is traveling forward on the helix, but the coupling coefficient should be no greater than that which makes the Kompfner wavelength four times the length of the helix. Otherwise, the pulse amplitude for this wave may be less than maximum. The Mod II extractor, to be discussed later, was conceived to overcome this problem, and more detailed discussion of the extractor behavior is presented in that context.

Throughout the period of study of the Mod I design, the only switch used was a spark gap in the form of a reed switch. The device used was the Clare RL 5480 reed switch. Its gas filling is hydrogen, at several atmospheres pressure, which, in conjunction with a supply of mercury which continuously wets the points, eliminates point erosion. One of the contact points is vibrated magnetically. Thus, a predetermined voltage can be applied to the antenna, which charges up to the full voltage early in the cycle while the points are far apart. When the points move together, the spark strikes, its voltage being repeatedly and precisely the preset value which is continuously adjustable from 0 to 4000 volts and directly measurable. (With a nonvibrating spark gap, the supply voltage--whether pulsed or steady--must be in excess of the spark voltage and there is always considerable difficulty measuring the exact spark voltage, which, incidentally tends to vary from pulse to pulse.) The spark-current rise-time determinations made with the Clare switch indicated 0.5 nanosecond. Effective rise times may have been much faster. The effective rise time was consistent over the entire voltage range, as indicated by the fact that the RF output was observed to vary as the square of the spark voltage. The main disadvantages of the Clare switch are its present limitations on

hold-off voltage (4000 volts, due to the insulation limit of the encapsulation), the limitation on vibration rate (60 cps), and its bulk. The physical size of the encapsulation and the long leads prevent incorporating the existing switch into a microwave Hertz resonator. These disadvantages could, however, be minimized to a considerable extent by an improved mechanical design. After all, the switch was originally designed for a much different purpose. It is, perhaps, surprising that it has served so well in the present studies.

For further work, there is the interesting possibility of incorporating the principal advantages of the reed switch in a Mod IV type of device. As detailed in later parts of this report, we have done considerable work using fixed-gap atmospheric discharges. In general, we have not found such gaps to be capable of consistently exceeding the performance of the reed switches, as measured by RF output at a given voltage or pulse-to-pulse reproducibility. We believe that the principles of (1) high pressure atmosphere, (2) mercury-wetted discharge electrodes which are, in consequence, self-healing, and (3) an externally driven oscillatory gap spacing can be very important, and that it is practical to obtain these advantages in a Mod IV type of design. Figure 10 shows one possible configuration.

Observations on the L-band converter included the following features:

- (1) Pulse envelope shape, viewed on sampling oscilloscope (HP 185B) and relatively slow (nominal rise time 35 nanosec.) conventional oscilloscope (Tektronix 535).
- (2) RF waveform, viewed on sampling oscilloscope and traveling-wave oscilloscope (Tektronix 519).



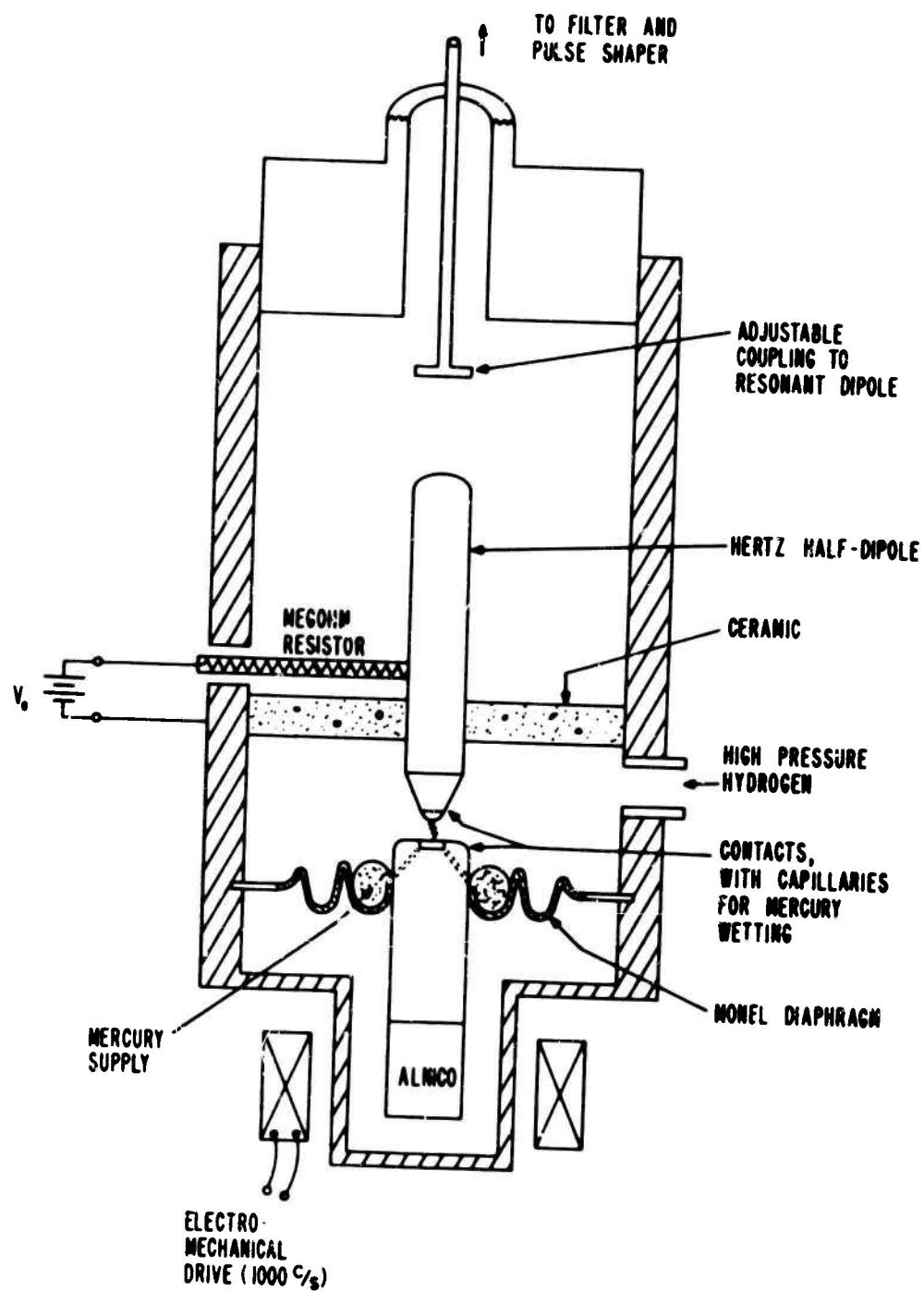
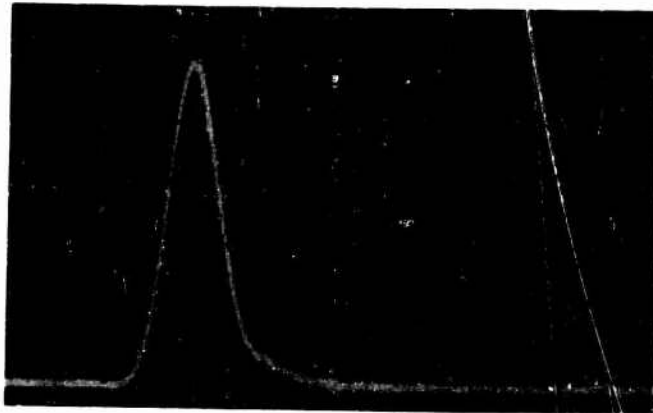


Fig. 10 Proposed Mercury-Wetted Vibratory Spark-Gap Design

- (3) Frequency spectrum, using a transmission-type wavemeter as an analyzer.
- (4) Peak pulse power, using a substitution method, against sources of comparison signals.

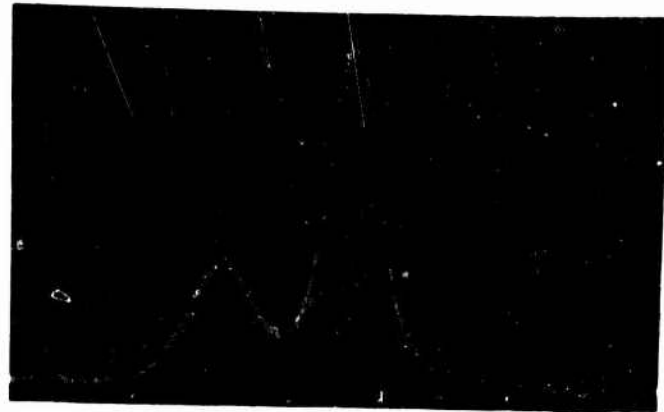
These observations may be summarized as follows: Envelopes of output pulses are shown in Fig. 11. At the switch end of the helix one extracts a single, strong pulse (at 1040 Mc) corresponding to "backward-wave" coupling between the fast wave and the helix wave. Depending on the response of the oscilloscope used, more or less detail in the envelope shape is seen. Small echoes suggest reflections from the helix supports. Periodic ripples on the pulse envelope (corresponding to frequencies of the order of 200 Mc) suggest multiple reflections of the fast wave (from the ends of the structure) and/or a (roughly) 200-Mc superposed oscillation of the spark current.

At the far end of the helix a weak, broad pulse (at 1270 Mc) is obtained first, corresponding to "forward-wave" coupling, followed, at the correct time interval, by an echo of the 1040 Mc "backward-wave" pulse described above. The "forward-wave" pulse is weak to begin with because its frequency is higher (see earlier discussions on spectrum of step function) and because the "forward-wave" coupling mechanism is a periodic function of coupling coefficient. (See the discussion in the next section of coupling in the meander-line structure.) Thus, the coupling to this wave could well be closer to a minimum than to a maximum, in view of the haphazard choice of coupling coefficient between helix and waveguide. Theoretical predictions that the "backward-wave" pulse should be asymmetrical, with a peak at the left, and that the "forward-wave" pulse should be square--though rounded by the effects of losses--appear to be confirmed by the oscillograms. (This feature is revealed even more clearly when using the meander-line structure--as described in the next section.)



(a) Backward Wave Pulse  
(40 nanosec./div)

(b) Forward-Wave Pulse (left)  
Plus Reflected Backward Wave  
Pulse (40 nanosec./div)



(c) Backward Wave Pulse (50 Mc Timing Wave)



(d) Forward Wave Pulse (left)  
Plus Reflected Backward Wave  
Pulse (20 nanosec./div)

Fig. 11 Output Pulse Envelope of Mod I Converter

(a) and (b) Using Tektronix 535 Oscilloscope

(c) and (d) Using H.P. Sampling Oscilloscope

Spectrum analysis of the two outputs showed that the RF energy was principally at the frequencies quoted, 1040 and 1270 Mc, the separation (20 percent) being the value predicted. Additional, weaker spectral components (or sidebands) were also present at separations of 50 to 100 Mc, or multiples thereof, from the main signal. They appear to correspond with the ripples on the pulse envelopes, and would thus represent superposed modulations due to wave reflections, or, perhaps more importantly, the low-frequency oscillations of the spark current revealed subsequently. The RF voltage waves themselves (Fig. 12) could be viewed with either of the high-frequency oscilloscopes to confirm the carrier frequency and modulation determined by other methods.

Reasonably successful attempts were made to sample the spark current, or its derivative, by bringing a suitable probe from the sampling oscilloscope into a hole in the coaxial line below the switch. The waveforms obtained (Fig. 13) revealed a sudden rise of current (taking approximately 0.5 nanosec.) followed by a damped oscillation at 43 to 66 Mc, depending on the length of cable between the switch and the antenna. This low-frequency Hertzian oscillation is thus associated with (and confined to) the conductors adjacent to the switch and very probably accounts for the observed modulations of the microwave output of the helix, though it cannot itself be propagated into the waveguide.

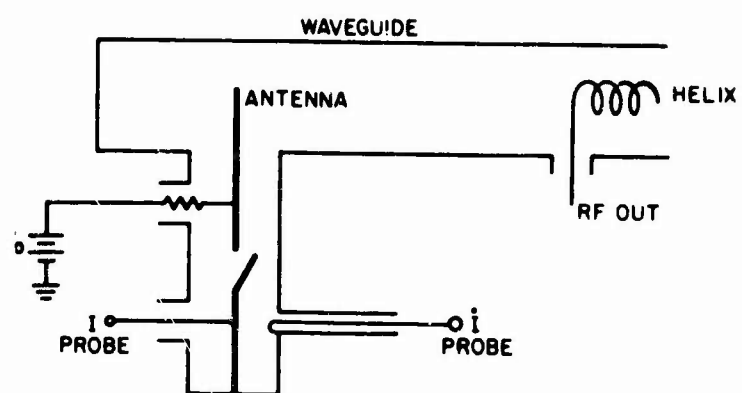
Measurements of RF power at the leading edge of the 1040-Mc pulse (averaged over the first 15 nanosec., approximately) indicate 0.2 watt per(kilovolt)<sup>2</sup> of applied voltage. This low figure reflects the haphazard choice of coupling coefficient between the helix and the waveguide. The power obtained from the S-band converters (Mod II and III) was considerably higher, because the coupling coefficient could be optimized, despite the fact that the higher frequency demands an a priori penalty of about one order of magnitude.



Fig. 12 RF Waveform (voltage vs. time) at Start of Output  
(Time scale: 1.0 nanosec./div)



(a) At 10 nanosec/div



(b) At 1 nanosec./div



(c) Derivative of Switch  
Current at 1 nanosec./div

Fig. 13 Switch Current Waveforms

In spite of its defects the L-band converter experiment, viewed in retrospect, appears to have been a good way of opening up the new subject and developing the first insights.

## 2. Mod II

The Mod II converter possesses a spark-gap exciter of one of several designs matched into a simple waveguide over a band of frequencies. From the waveguide, a reflectionless, frequency-sensitive, directional coupler extracts a still narrower band of frequencies, energy at the unused frequencies being absorbed in a termination beyond the directional coupler. Although this latter energy is intentionally absorbed, a Mod II converter need not have a lower overall efficiency than a converter in which it is reflected: In a short-pulse system reflected energy is not readily reconverted, but must rather be dissipated eventually through multiple reflections. The principal virtue of the Mod II arrangement which separates the extractor and exciter by a connecting guide having simple and well known characteristics, is that it makes it easier to study the extractor and the exciter (the latter is the more difficult) independently.

The most reproducible data were taken with an exciter containing the mercury-wetted reed switch (Figs. 14 and 15) as a spark gap. Because of the vibrating armature, this switch can have any accurately preset firing voltage from 0 to 4000 volts without much influence on the already short rise time. The result is that RF output power could be depended on to vary as the square of the firing voltage. The antenna was matched to the waveguide over S-band. The piston below the switch capsule is intended to help adjust the length of the coaxial portion to be half a Hertz-dipole, and on to vary the relative

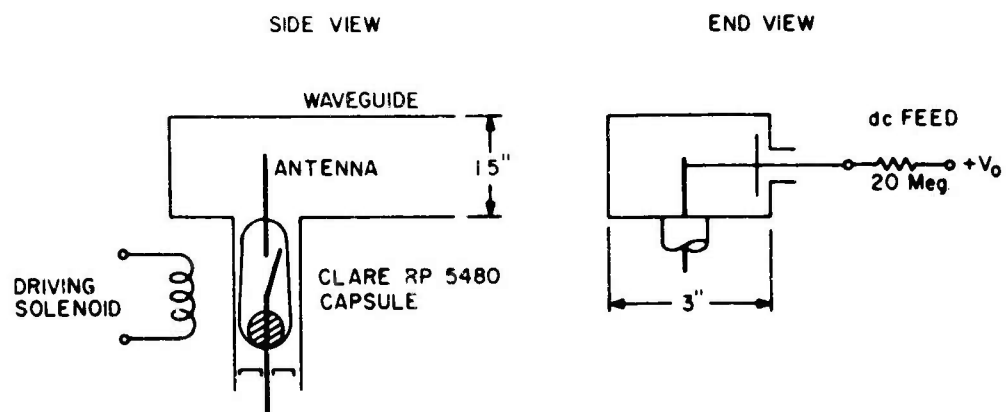


Fig. 14 Waveguide Exciter for Mod II Converter

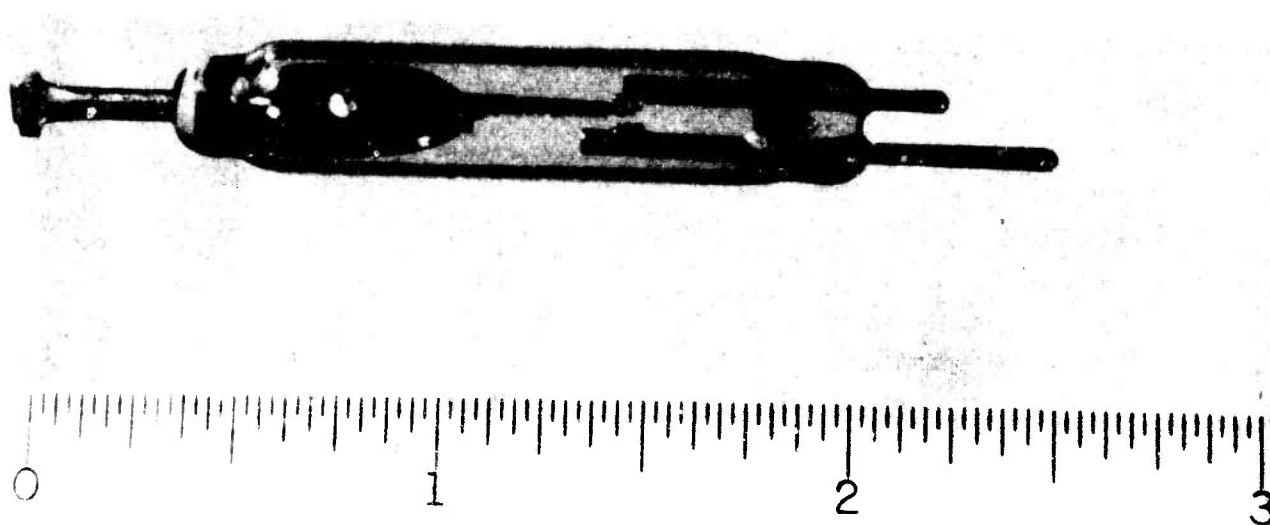


Fig. 15 Photograph of Mercury-Wetted Reed Switch (Clare RP 5480)

Switch closes when arm moves from short electrode (which is not used) to longer electrode which leads to the waveguide antenna.



position of the spark gap along such a dipole. In practice, however, the effect of this piston on RF output is no more than  $\pm 1$  db. The antenna is charged through a thin wire that does not seriously perturb the fields in the waveguide.

Our frequency-sensitive direction-coupler is novel. It consists of a flat "meander" line of 100 periods inside the rectangular waveguide (Fig. 16). (Its width is 2 inches and there are 2 periods per inch axially.) The meander strip is suspended in the waveguide between the broad walls, with the ends connected to coaxial fittings brought out through the narrow walls. The match at these two ports is refined with stub tuners (Fig. 17). The frequency (roughly 3000 Mc) at which coupling nominally should occur corresponds to synchronism between RF fields in the guide and on the meander line. This condition corresponds to the developed length of a repeating section equal to  $\lambda_0$ . When the plane of the meander is horizontal, the coupling is nil because there is no component of waveguide E-field along the bars. As the plane is tilted (by means of small dielectric supports and levers inside the guide) the coupling coefficient increases monotonically.

Two kinds of coupling can be predicted, according to the relative directions of the two waves. For "counter-flow" coupling, the frequency of maximum transfer is below the nominal coupling frequency (a Doppler shift, but reckoning with the opposed group and phase velocities of a meander line) and the transfer should increase monotonically with angle of tilt ( $\theta$ ). Cold testing revealed that the frequency in question was near 2410 Mc, and that the insertion loss (waveguide input to upstream coaxial terminal) did decrease monotonically with  $\theta$ . Transfer should be essentially complete for  $\theta$  of the order of 15 degrees, but in practice, insertion loss continues to decrease

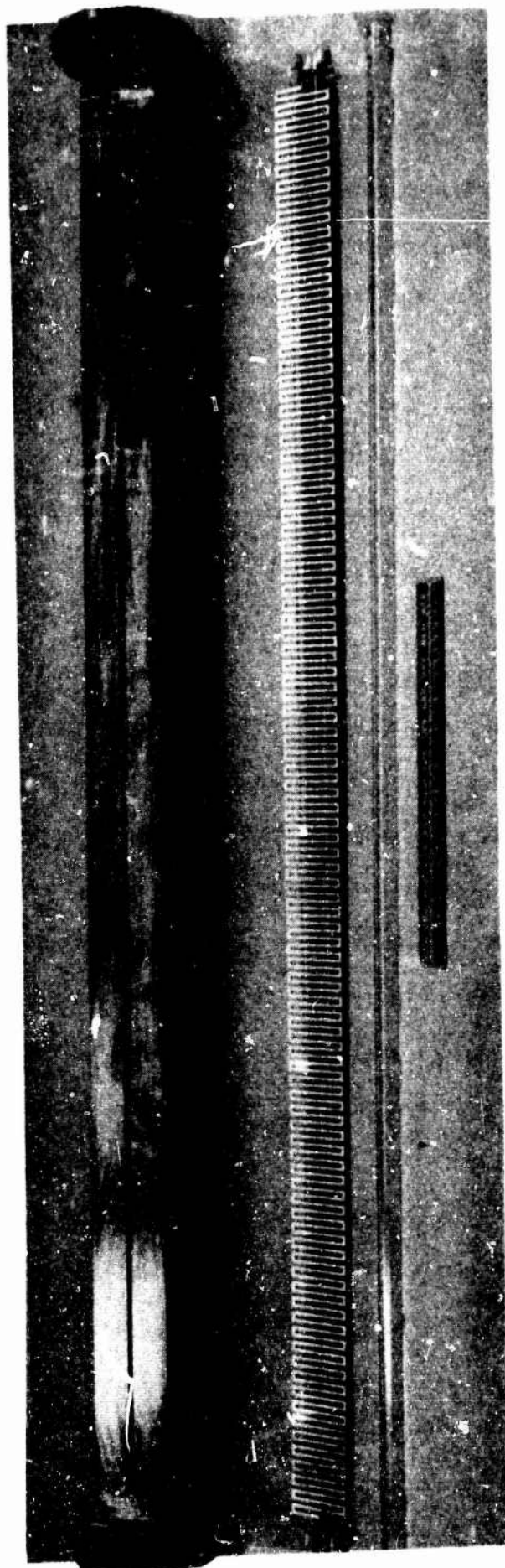


Fig. 16 Components of Mod II Extractor

past this angle. This result is due to ohmic losses: increased  $\theta$  diminishes the length of meander line needed to accomplish transfer, and thus the accompanying ohmic losses.

For "co-flow" coupling (waveguide input to downstream coaxial terminal), the critical frequency is raised, to 3160 Mc. In this case, energy oscillates back and forth between the coupled lines at a rate which increases with  $\theta$ . The result--as is readily confirmed by cold test--is that for  $\theta = 3^\circ$ , energy passes just once from guide to meander. At  $\theta = 6^\circ$ , it has passed entirely back to the guide, and so on. Thus we find the insertion loss to be infinite at  $\theta = 0, 6, 12, 18^\circ, \dots$ , but less than 1 db at  $\theta = 3, 9, 15^\circ, \dots$ .

A spurious low-frequency coupling near 2150 Mc was identified as involving the end bar of the meander line, at a frequency determined by the waveguide cutoff and not the meander line itself. To avoid contamination of data by this spurious response, all observations of RF output were made with high-pass filters cutting off at a frequency at least as high as 2300 Mc.

To summarize, the extractor described is very versatile. It provides two types of coupling, at different frequencies, with continuously variable coupling coefficients. For an impulse type of input, these variable coupling coefficients can control the length and shape, as well as the amplitude, of the output pulse envelope. Performance was predicted as follows:

When an impulse containing energy over a broad band of frequencies enters the waveguide at the left (Fig. 17), a burst of power at 3160 Mc should be obtained at the right-hand coaxial output after a few nanoseconds delay. Ideally, this "forward-wave" pulse would be square and 100 periods

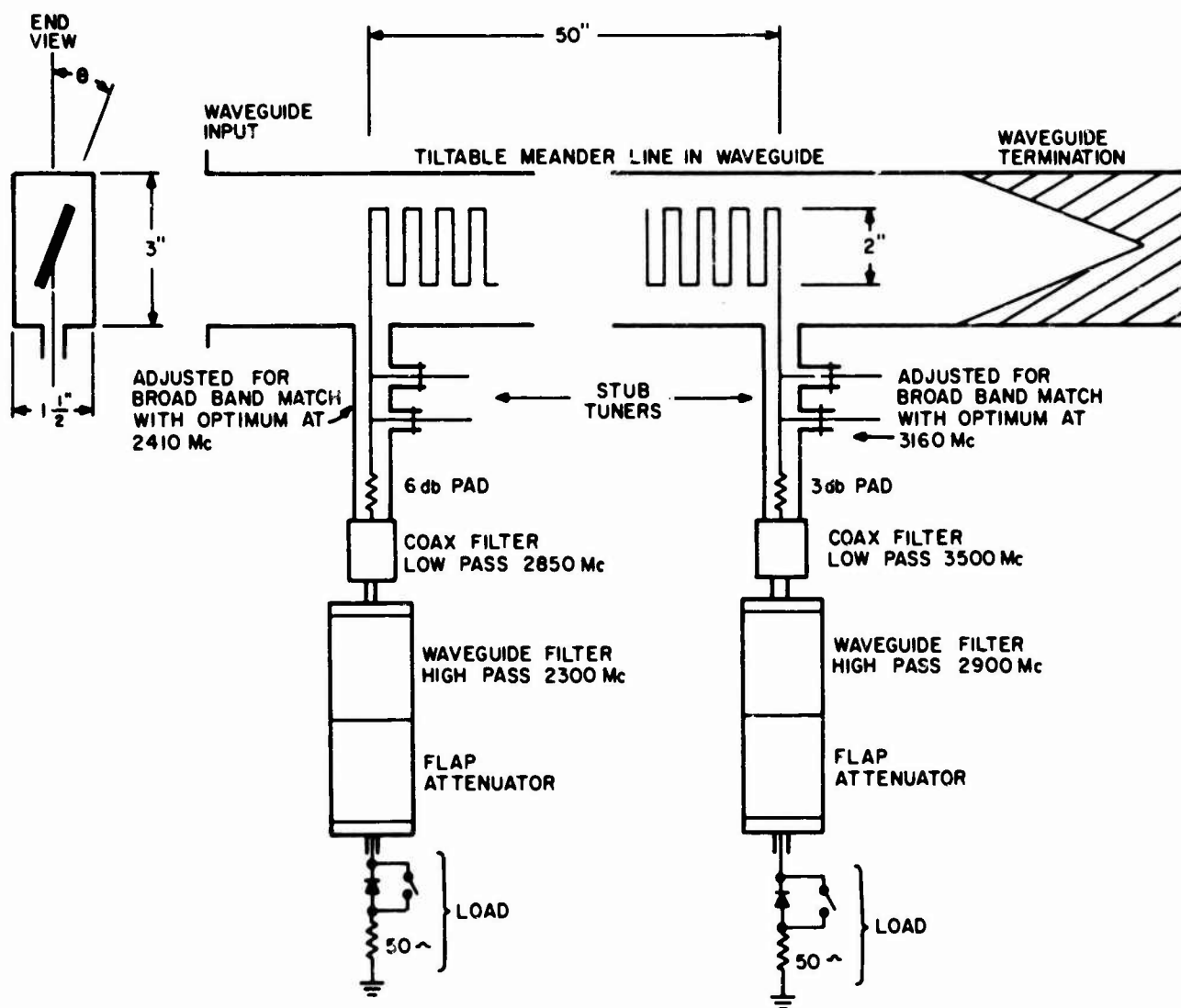


Fig. 17 Schematic Diagram of Mod II Extractor and Test Equipment

(approximately 32 nanoseconds) long. The amplitude would vary cyclically with  $\theta$ , being a minimum at  $\theta = 0, 6, 12, 18, 24$  degrees, approximately, and a maximum at  $\theta = 3, 9, 15, 21, 27$  degrees. A few nanoseconds sooner, a burst of "backward-wave" power at 2410 Mc would begin to be obtainable at the left-hand coaxial output. This pulse envelope has a tall leading edge and decays exponentially. As  $\theta$  increases, the pulse becomes narrower and much taller. Both the peak power and total pulse energy increase monotonically with  $\theta$ , though the effective pulse length decreases.

These predictions were confirmed when the exciter and extractor units were combined.

The envelope of the forward-wave output pulse at  $\theta = 3^\circ$  (first maximum) is shown in Fig. 18. (The crystal detector was operated in the linear, rather than the square-law, region so that the ordinate is proportional to voltage rather than power.) The peak power is 1.3 watts at  $V_0 = 4000$  volts. The frequency is 3160 Mc and the phase of the RF wave within the pulse remains fixed relative to the rise of current in the spark (Fig. 19). The variation of output with angle of tilt is recorded in Fig. 20. The several minima are finite rather than zero because of a finite frequency spread in the output spectrum. Power transfer in the coupler is frequency-sensitive so that the minima would be zero only if the signal were of a single frequency.

The forward-wave performance does not wholly conform to theory in that the output pulse width is shorter than expected by almost 50 percent. An explanation is still being sought. It may be a consequence of the fact that the theory has so far been worked out only on a single-frequency basis, whereas the driving signal is actually spread out over a broad band. The rounding of the corners of the pulse could be due to the effects of ohmic losses.

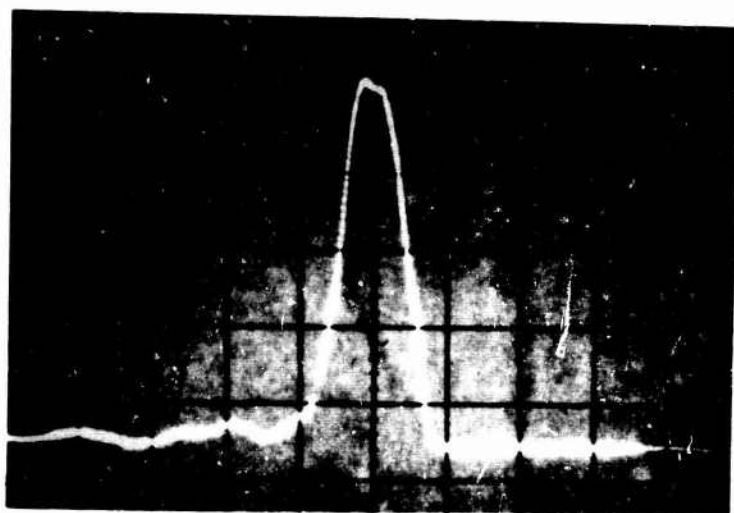


Fig. 18 Voltage Envelope of Forward-Wave Output Pulse ( $\theta = 3^\circ$ )

(Hewlett-Packard 185B Sampling Oscilloscope)

Vertical: 50 mv/div

Horizontal: 10 nanosec./div

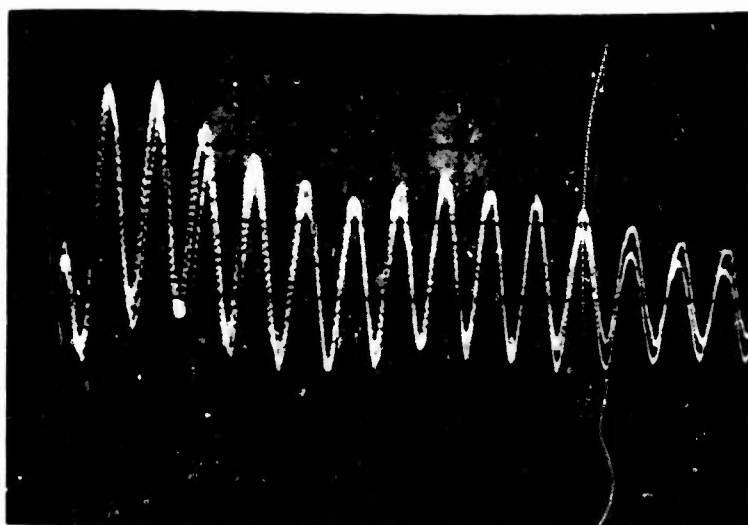


Fig. 19 RF Waveform of Forward-Wave Output Pulse ( $\theta = 3^\circ$ )

(Sampling Oscilloscope)

Vertical: 20 mv/div

Horizontal: 0.5 nanosec./div

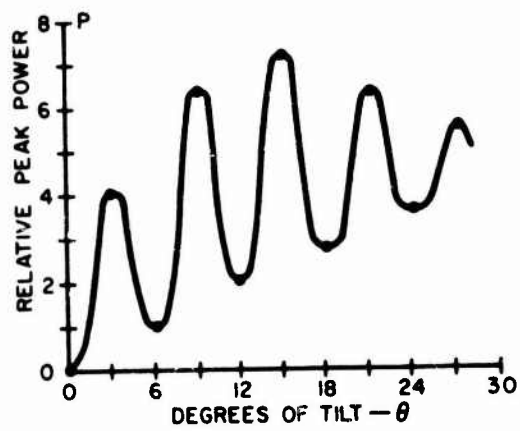
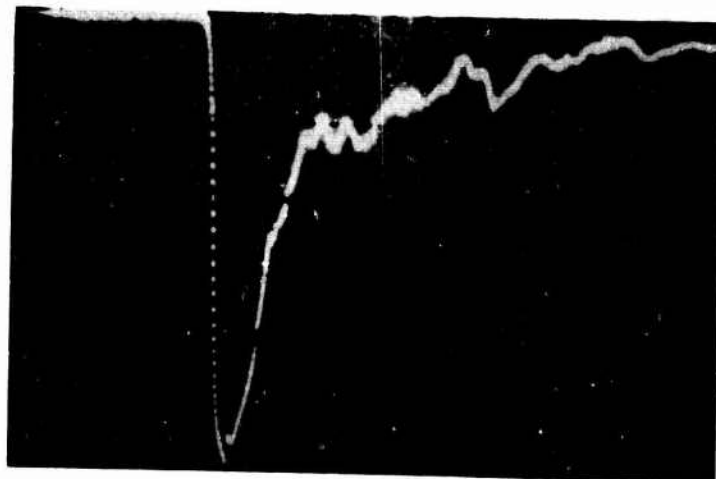


Fig. 20 Variation of Output Power with Angle of Tilt for the Forward-Wave Pulse

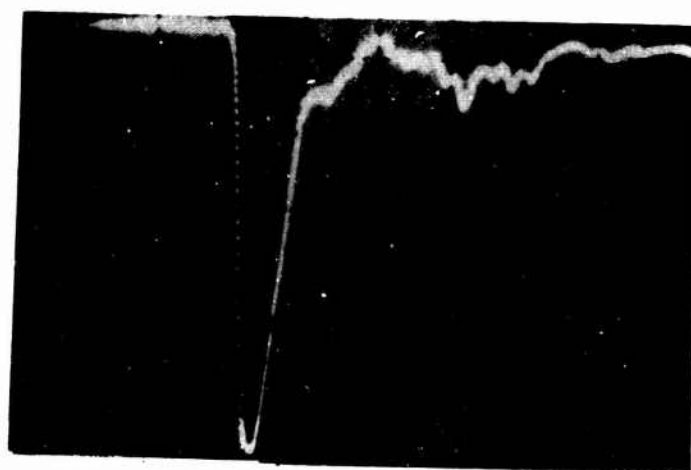
The envelope of the backward-wave output pulse is shown in Fig. 21. The envelope shape is close to that expected, and the narrowing of the pulse toward the leading edge as  $\theta$  increases is in agreement with theory. That is, at large  $\theta$  almost all the power is extracted close to the left-hand end of the meander line. The oscillograms of Fig. 21 have been normalized by inserting attenuation; in actuality, the peak power level increases rapidly with angle of tilt, as shown in Fig. 22. At  $V_0 = 4000$  volts, peak powers (at 2410 Mc) of 35 watts at  $\theta = 20^\circ$  and 54 watts at  $\theta = 25^\circ$  are obtainable. The fact that there is so much more power available in the backward wave than in the forward wave is mainly a result of the lower frequency of the former. The voltage spectrum of the spark current transient decreases very rapidly with frequency for many reasons, including finite rise time.

These S-band signals can be resolved with the 185B sampling oscilloscope, bypassing the crystal detector (Fig. 23). A more conventional oscilloscope can also be used to advantage: The Tektronix 535 has a rise time of 35 nanoseconds, so that when the crystal detector output is fed into it, the pulse seen (Fig. 24) shows little detail and is broader than the true pulse. In fact, the slow oscilloscope produces a pulse whose height seems to be very nearly proportional to the average height of a very short pulse like that of Fig. 21(c). That is, the height of the pulse of Fig. 24 is approximately proportional to the integrated power--or the energy--of the original pulse. Based upon this assumption, the variation of pulse energy with angle of tilt was determined and recorded in Fig. 25. The increase of pulse energy with  $\theta$  beyond the point where  $\theta$  is sufficient for complete power transfer is a result of pulse sharpening: A shorter pulse (in the time domain) has a broader spectrum (in the frequency domain) and therefore utilizes more of the output of the spark gap, which has a very wide spectrum indeed.





(a)  $\theta = 5^\circ$



(b)  $\theta = 12^\circ$



(c)  $\theta = 24^\circ$

Fig. 21 Voltage Envelope of Backward-Wave Output Pulse at Increasing Angles of Tilt (Increasing attenuation is inserted to normalize amplitude)

Vertical: 50 mv/div

Horizontal: 10 nanosec./div

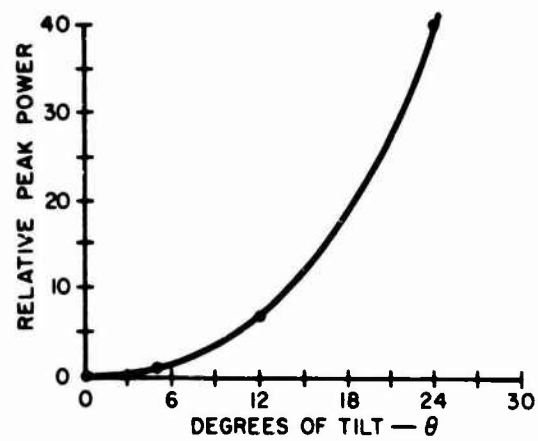


Fig. 22 Variation of Peak Output Power with Angle of Tilt for Backward Wave (2410 Mc) Output of the Mod II Converter

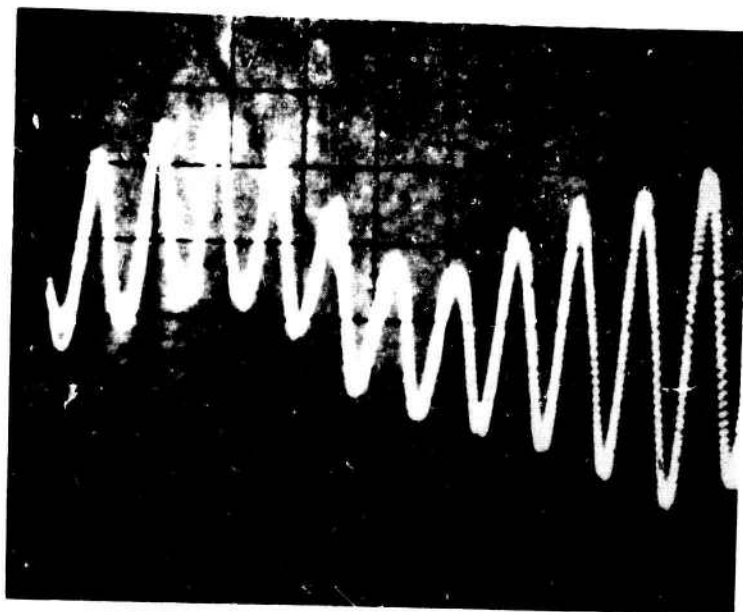


Fig. 23 RF Waveform of Backward-Wave Output as Seen with Sampling  
Oscilloscope ( $f \sim 2400$  Mc)  
Vertical: 50 mv/div  
Horizontal: 0.5 nanosec./div

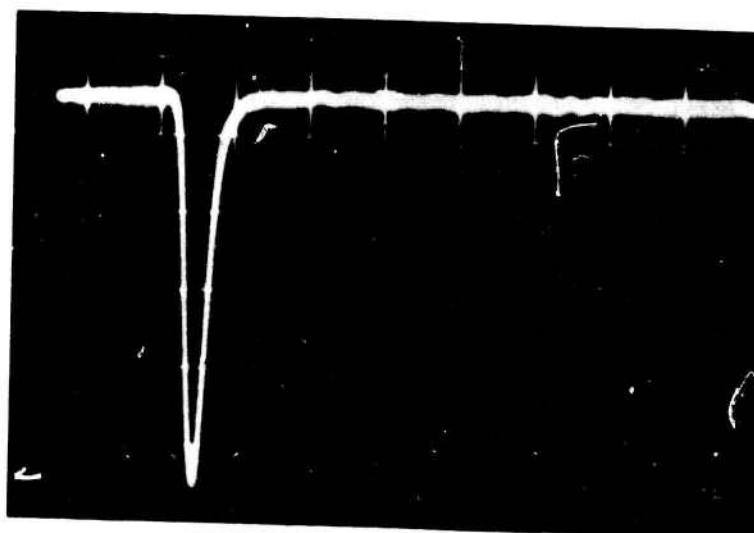


Fig. 24 Voltage Envelope of Backward-Wave Output Pulse as Seen with  
Tektronix 535 Oscilloscope, Model K "Plug In"  
Vertical: 50 mv/div  
Horizontal: 100 nanosec./div

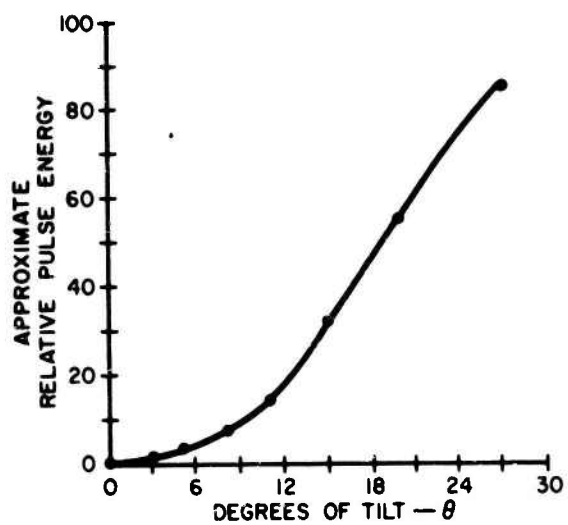


Fig. 25 Variation of Pulse Energy with Angle of Tilt for Backward-Wave Output Pulse

### 3. Mod III

The Mod III device consisted of an S-band waveguide filter with the spark gap in the first section. This model provided a convenient system for the exploration of the effects of various spark-gap configurations and of various charging circuits.

The general design used is shown schematically in Fig. 26. The back plunger and the gap position and spacing are adjusted to optimize the amplitude of the RF output pulse.

The choke was designed to appear as a short-circuit to the spark gap at the operating frequency. At frequencies far from the operating frequency, it ceases to be an effective choke. At low frequencies, the choke acts essentially as a simple capacitance in series with the inductance of the electrodes and the discharge, so that a low-frequency resonance can be expected in the system. Figure 27 shows this effect; the waveform of the discharge current was recorded by a sampling oscilloscope after replacing the bottom electrode in Fig. 26 with a high-frequency resistance of the type shown in Figs. 28, 29, and 30. In these elements, the plain electrode is replaced by a coaxial line connected to the oscilloscope and shunted at the end nearest the discharge by either a metallized disc or by a group of fine wires arranged radially. The resistance in each case was about 0.03 ohm initially. The resistance of the metallized disc, however, gradually decreased to about 0.01 ohm with use. In both cases, an accurate picture of the current waveform should be obtained because the resistance is very much less than that of the coaxial line (nominally 50 ohms) and because the inductive reactance of the shunt is believed to be essentially negligible.

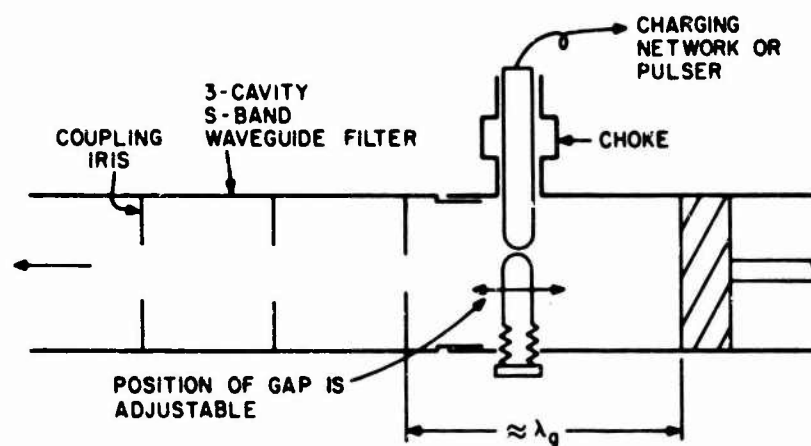


Fig. 26 Schematic Diagram of Mod III Converter

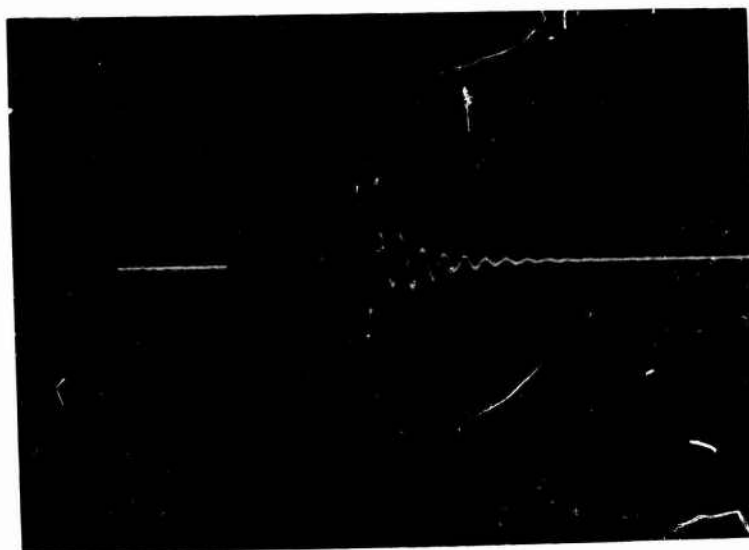


Fig. 27 Oscillogram of Current Waveform in Discharge Using the Radial Wire Probe of Fig. 30, and the Sampling Oscilloscope (Hewlett-Packard 185B). The high-potential electrode was charged positive.

Vertical: 0.2 mv/cm

Horizontal: 10 nanosec./cm

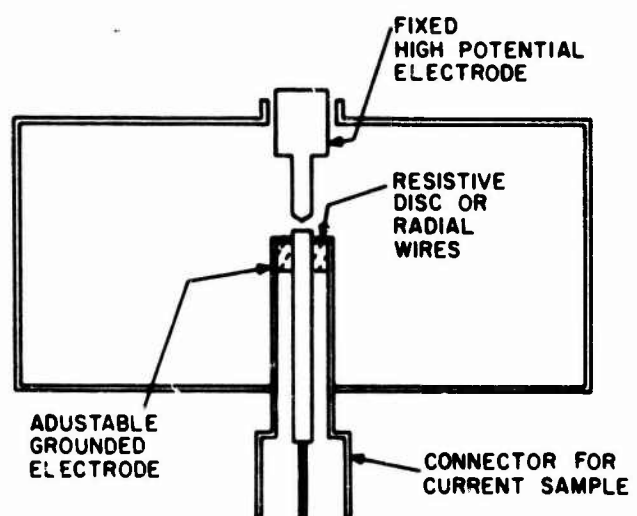


Fig. 28 Sketch of Current Sampling Probe

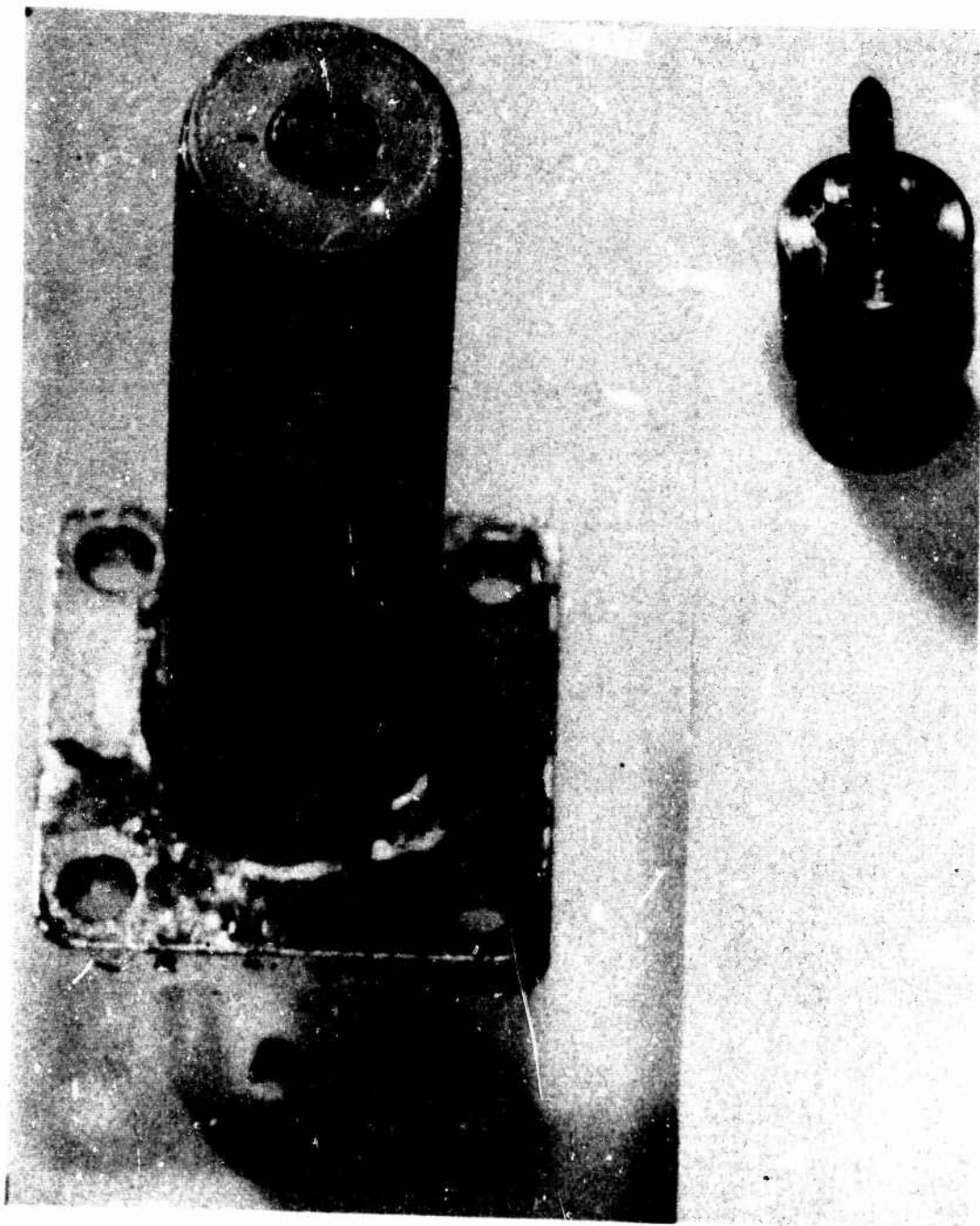


Fig. 29 Photograph of Resistive-Disc Electrode



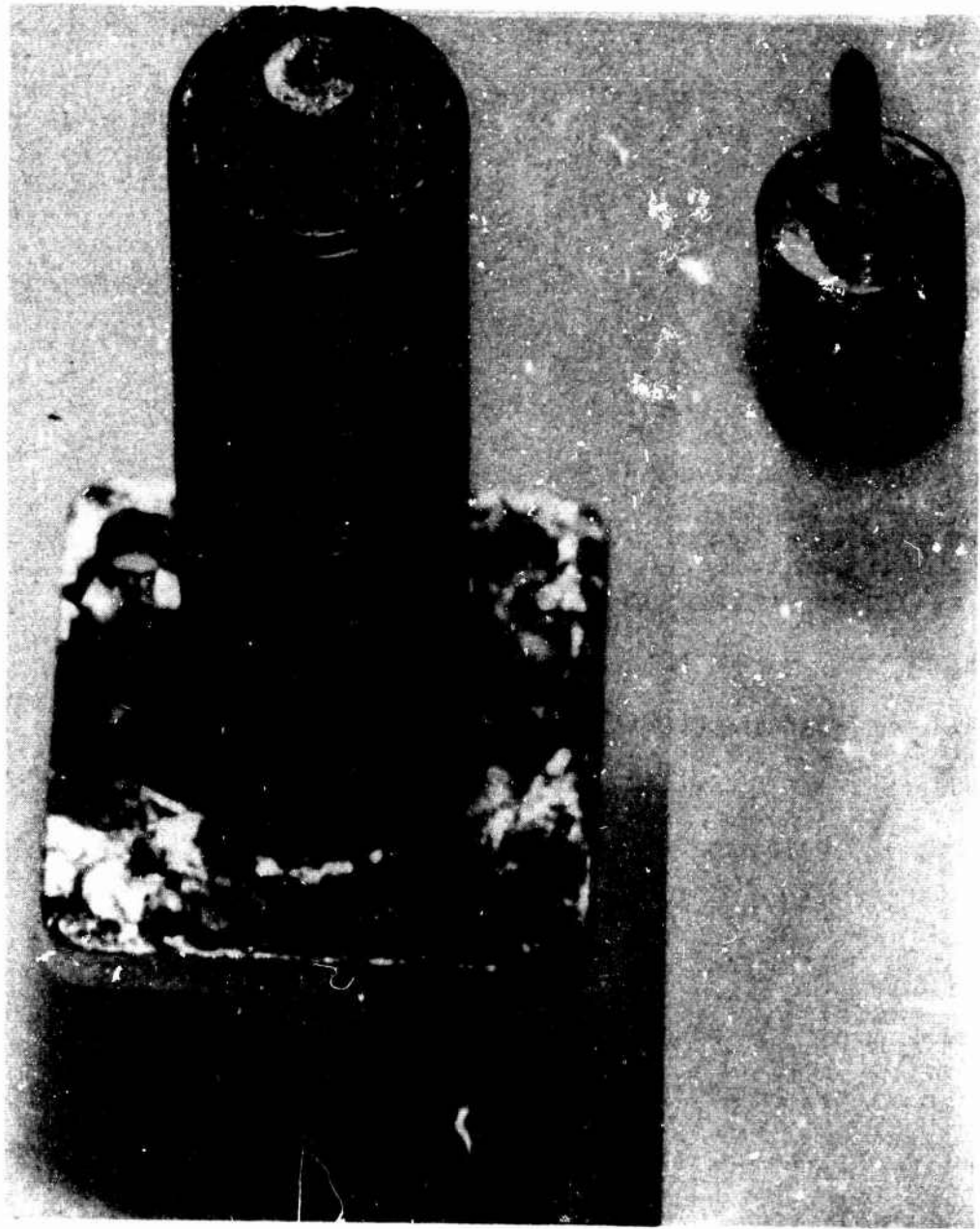


Fig. 30 Photograph of Radial-Wire Resistive Electrode

The oscillation recorded in Fig. 27 is at about 400 Mc, which seems a reasonable value. This low frequency oscillation has several undesirable effects. First, it represents energy that is dissipated mainly in the discharge and hence lowers the efficiency of the device. Also, it contributes to the erosion of the electrode points. There is some evidence, in fact, that it is the principal cause of the observed electrode erosion. Finally, the most significant effect for our immediate purposes was that this large oscillation effectively masked any direct and unambiguous observation of the Hertz effect at or near the microwave frequency of interest.

We also made some preliminary experiments with a system in which the RF choke was replaced by a helix of fine wire with the charging resistance at the electrode end. These elements were arranged to have minimal effect on the RF field in the cavity. While some mechanical problems remain, it appeared that this arrangement did eliminate the choke resonance effect.

A variety of electrode designs were studied, some of which are shown in Fig. 31. The configuration of Fig. 31(b) was used in an effort to reduce the impedance of the discharge. It was hoped that the two gaps would be sufficiently strongly coupled optically so that they would fire simultaneously. This did not seem to be the case, but it was found that the second parallel electrode was effective as a tuning adjustment to increase the RF output. This was confirmed with the configuration of Fig. 31(c) in which there is no optical coupling between the gaps.

The design of Fig. 31(d) was used as a more predictable form of tuning. In effect, the electrode is built into a section of coaxial line, short-circuited on one end, and capacitively tuned at the other. This electrode design may be considered as the precursor of the Mod IV system design.

The configuration of Fig. 31(e) was built to check some of our ideas regarding the possibility of using multiple gaps in series. In the particular system being studied, it did give nearly four times the RF power of a single gap, and operated at about twice the voltage.

The Mod III assembly did provide a good system in which to make the preliminary studies of the effect of gap design. For some applications, where a particular pulse shape may be specified and where a compact system is desired, it seems to offer considerable advantages.

#### 4. Mod IV, Preliminary Design and Measurements

As discussed earlier, Hertz boosting could have a substantial effect on the power output of our converters. In our previous experiments, there was always doubt as to whether a resonance at a sufficiently high frequency could exist for the spark current, whether or not superposed on a stronger, lower-frequency oscillation. When the spark current could be monitored, it was usually found to be oscillating strongly at frequencies as low as a few tens of megacycles per second, as determined by the inductance and capacity to ground of the lead between the "hot" electrode and the charging resistor. In cases where the charging resistor was connected directly to the "hot" electrode, the electrode itself was much longer than one-quarter wavelength at the frequencies of interest. We therefore feel we must now take stronger measures to be sure of forcing the spark current into a Hertz oscillation at the kilomegacycle frequency of interest. If we succeed, we can add a suitable pulse-shaping band-pass filter centered at the same frequency. (The filter here should absorb, rather than reflect, unwanted frequencies to avoid "pulling" the resonance of the Hertz dipole.)

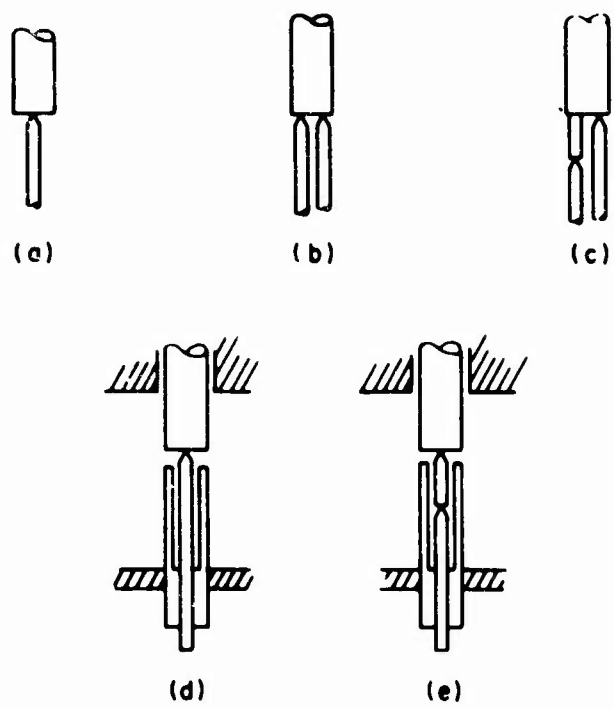


Fig. 31 Electrode Designs

The proposed Hertz oscillator, on which preliminary data was obtained, is essentially as shown in Fig. 32. It differs from the classical sparked dipoles in being unbalanced, and completely shielded with a variable output load coupling. (In addition to loops, E-probes and irises in the shield wall should also make satisfactory adjustable couplers which do not affect the original resonant frequency.) The resistor for applying voltage to the "hot" electrode merely has to have a value high enough not to affect the loaded  $Q$  of the resonator. In our test (see the photograph of the cavity, Fig. 33) with resonance at 2650 Mc, the "cold"\* unloaded  $Q$  was 200 and a 0.1-megohm resistor was sufficiently large. Depending on how low the "hot"<sup>†</sup> loaded  $Q$  might be in practice, a smaller resistor could be used. This may be desirable if, instead of dc, or slow-rising pulses, the "hot" electrode is to be fed with semi-fast-rising impulses; i.e., impulses whose rise time is less than the "statistical time"<sup>15</sup> of the gap in the dipole. (Since the capacitance of the rod is only a few picofarads, a resistor as large as 10,000 ohms will still preserve rise times as fast as 100 nanosec, an interval quoted as being short compared to the "statistical time.") It is to be noted that this cavity cannot possibly resonate at a frequency lower than that for which the rod is one-quarter wavelength long, modified only by spark inductance, fringing capacity at the upper end of the rod, and dielectric loading of any plastic or ceramic structure used to support the rod or the resistor. (It is conceivable that this same resonant frequency could be obtained as a higher-order resonance of a longer rod. But then, however,

---

\*i.e., with the gap electrodes touching.

†i.e., with the gap open and firing.

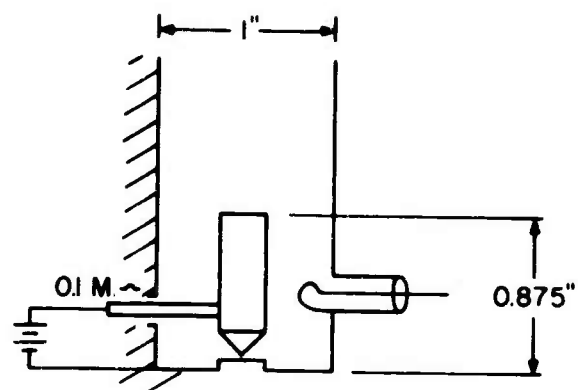


Fig. 32 Unbalanced, Shielded Hertz Oscillator

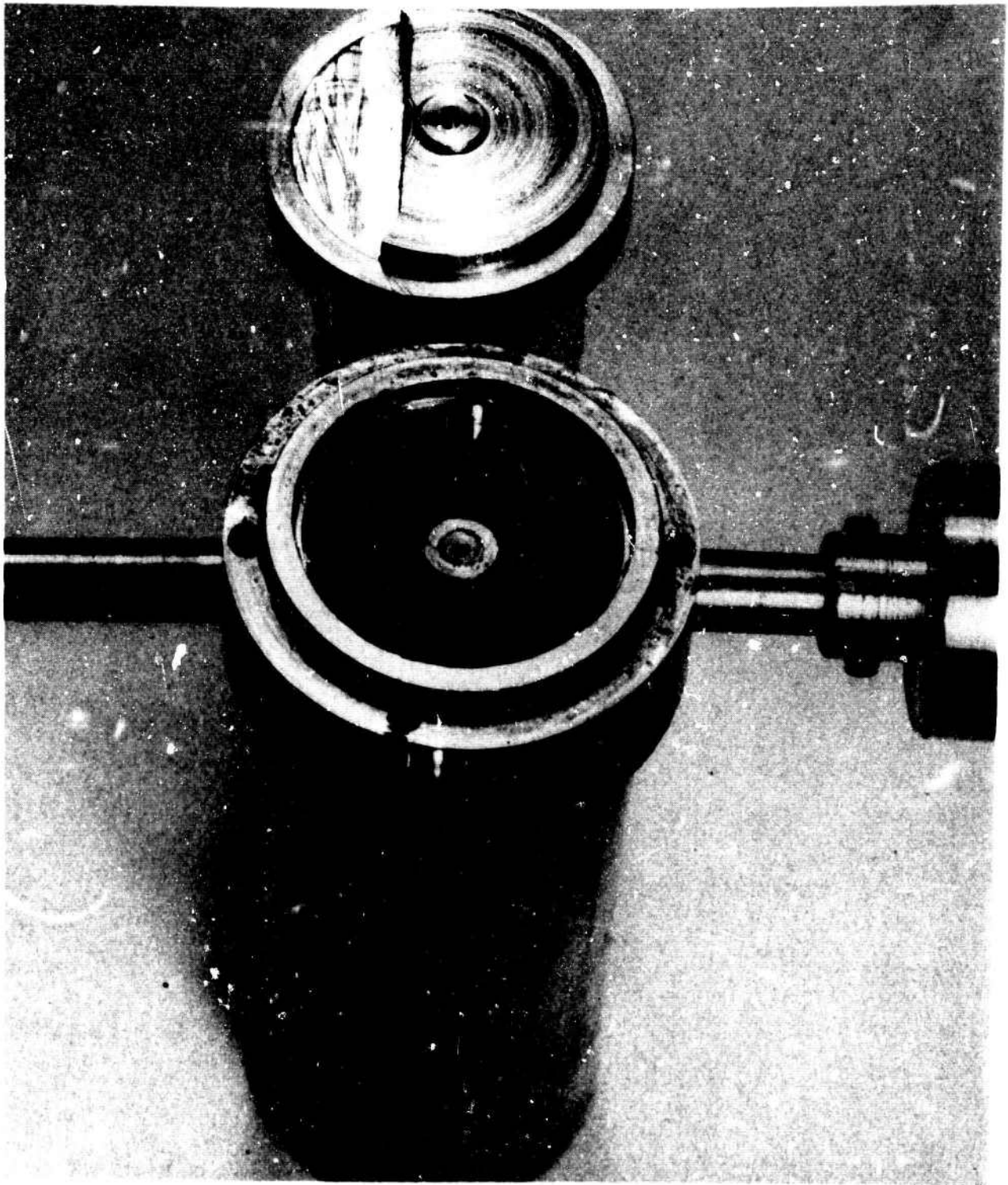


Fig. 33 Photograph of Mod IV Cavity Used

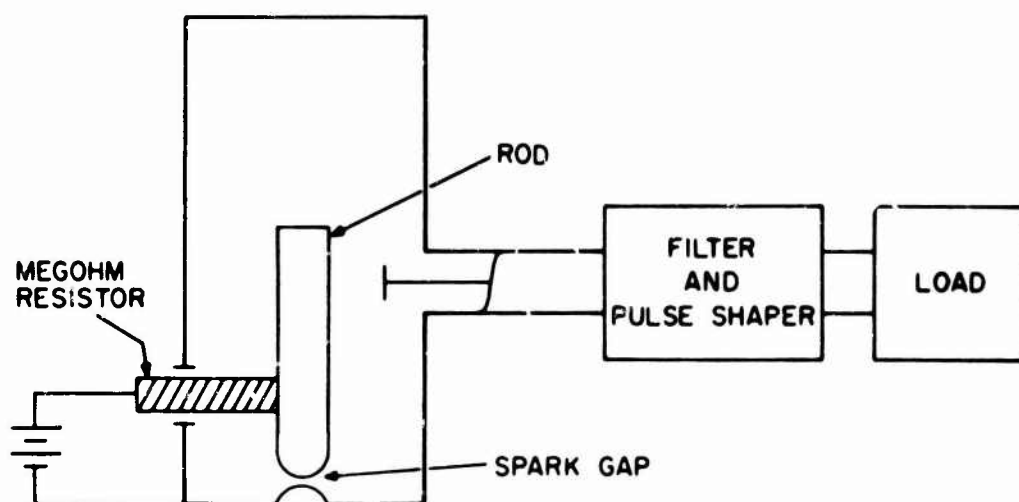


Fig. 34 Schematic Diagram of Proposed Mod IV Converter



the greater quantity of charge oscillating in the fundamental resonance would obscure any weaker oscillation and prevent its observation, and also uselessly erode the points. In addition, one could not be altogether sure of the partition of energy among the several resonances. Perhaps, but not necessarily, the energy driving the higher-frequency oscillation might be limited to that stored only on the part of the rod next to the gap and extending back a distance of one-quarter wavelength at the higher frequency.)

When the Hertz oscillator of Figs. 32 and 33 was set up, the position of the loop corresponding to critical coupling of the "cold" cavity was noted, and the loop was then pushed in a little farther, which was as far as it could go. The loaded  $Q$  then would have been of the order of 50, neglecting resistance in the spark. With the spark operating at atmospheric pressure, and voltage and gap spacing optimized for maximum power output, the spectrum of the RF output was as plotted in Fig. 35. This curve indicates a loaded  $Q$  of only 5, approximately, according to the half-power points.

The crucial question here is the reason for this drop in the apparent  $Q_L$ . At least three explanations are possible:

- (1) The drop may be real and due to resistive loading by the spark resistance.
- (2) The spread of the spectrum may be due to a random variation of the tuning from pulse to pulse due to variation of the inductance of the arc, which is in series with the rod.
- (3) The spread may be due to a frequency modulation within each pulse due to a variation with time of the inductance of the spark.

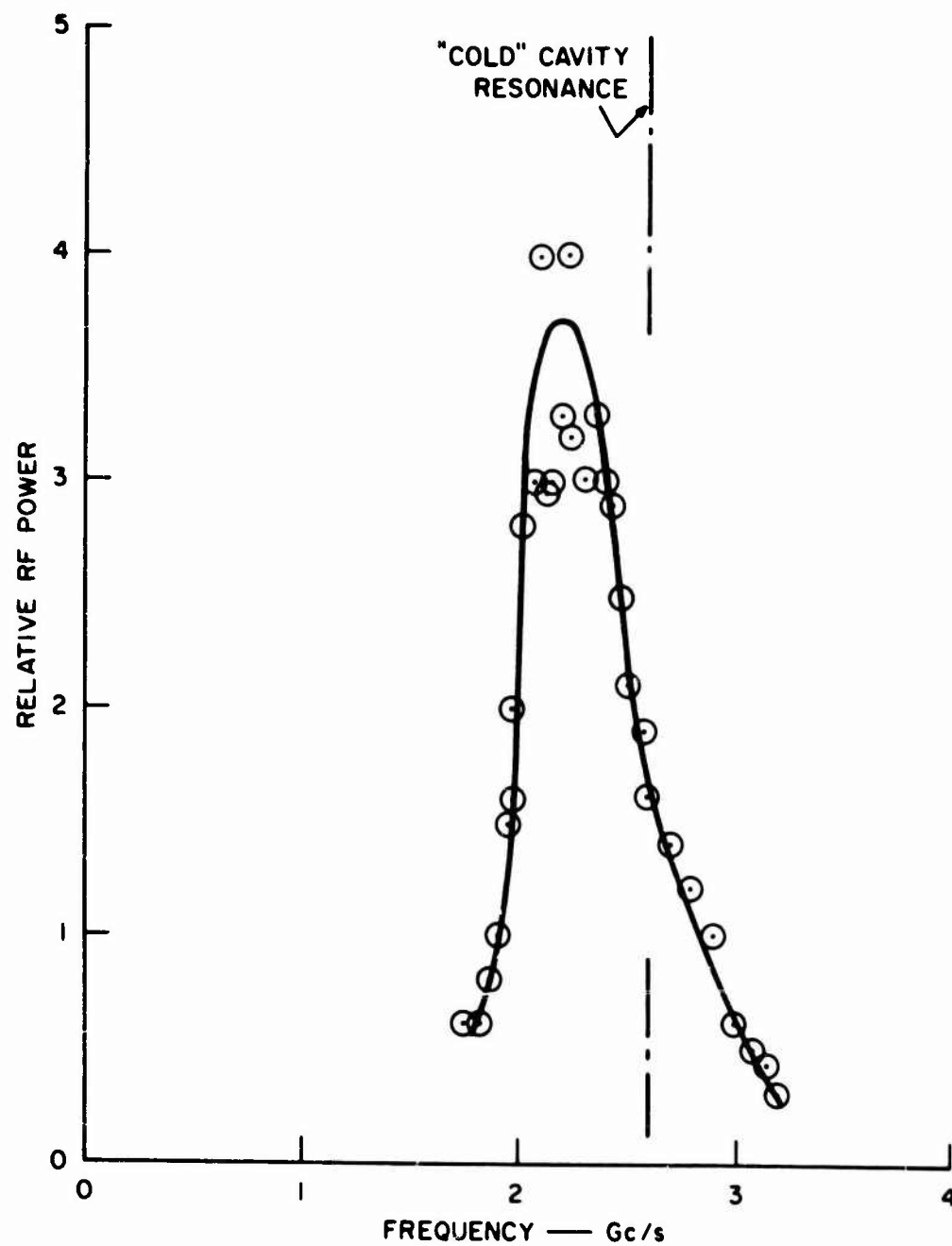


Fig. 35 Output Spectrum of Mod IV Converter Cavity (Without pulse-shaping filter)

We may also note that the spectrum peak in Fig. 35 is shifted significantly downward from the "cold" resonance (obtained with the spark-gap short-circuited.) This indicates that the inductance of the spark is indeed significant. Since there appears to be no reason to expect that this inductance would be constant during the first few cycles of the RF, we think it likely that significant frequency modulation within the pulse did occur.

Much more detailed study will be necessary to determine which of these mechanisms--or what combination of them--is responsible. The distinction is important since it affects the possible efficiency of the system, and will determine the possible effectiveness of what we have called the Hertz effect.

The advantages of this type of system appear to be substantial. The complete suppression of all lower-frequency resonances means that all of the stored energy must become involved with the generation of the desired RF. If the spark gap were lossless, and there were no other losses in the system, the efficiency would be 100 percent. (With the resistive charging indicated, there is charging loss, but this might be avoided by using resonant charging.) Also, the only currents through the spark are those that contribute directly to the output. This minimizes erosion effects on the spark geometry, which becomes a very important factor at high powers.

The Mod IV concept also gives us the chance to separate the RF-generation function from the pulse-shaping function in order to better understand the former. (Later, they might be recombined.) In addition, the cavity with the half-dipole is especially amenable to the various schemes needed to increase the hold-off voltage of the gap without prolonging the rise time of the discharge once it starts. These schemes include pressurization, liquid filling,

gap vibration ("reed-switch" effect), disposable dielectric tapes, etc., as described elsewhere.

Much further work is needed to explore these possibilities and to determine the capabilities of this type of approach. However, it is evident that the Mod IV design is one that is worth careful attention.

#### 5. Supplementary Spark-Gap Studies

In view of the complex interactions between the various parameters of a spark gap, it was decided to take a series of measurements in which the RF structure remained fixed while a minimum of spark gap parameters were varied in a simple manner. These measurements were limited to atmospheric gaps with copper-tungsten electrodes. The RF extractor was the Mod II meander line in which all geometric settings remained fixed throughout the experiment. The pulse energy output at the "backward-wave" connector was observed on the "slow" oscilloscope, with the pulse height kept constant (to avoid detector nonlinearity) by insertion of a variable attenuator. The attenuator setting is reported as "relative RF output." The gap width was the principal independent variable. Turning a micrometer screw allowed the electrodes to touch and then be separated. The micrometer reading is reported as "gap spacing," although the error at spacings of only a few thousandths of an inch may be considerable due to imperfect concentricity and other mechanical imperfections. With wider gaps, the error is less significant. Some data with electrode shape as an independent variable were also recorded.

In addition to RF output, breakdown voltage and rise time were independent variables. The latter quantity was observed as the "10%-90%" rise time of the step observed in the output of a current probe (the multiwire probe of Fig. 30)

applied to a sampling oscilloscope. The stray inductance of this probe may introduce error into the measurement, especially at the shorter rise time. When the supply voltage was applied to the spark gap in the form of microsecond pulses at a kilocycle repetition rate, the breakdown voltage was indicated directly on an electrostatic peak reading voltmeter. When the spark gap was fed from a dc supply through a charging resistor, this voltmeter could not be used. Since the ensemble is a relaxation oscillator, however, the breakdown voltage could be measured with reasonable accuracy by recording the supply voltage at which the device ceases to operate.

In view of the imprecision described, the data which follows should be regarded only as indicating trends and gross effects. This work should be considered only as a preliminary to the measurements that would be needed for a thorough study of gap design and behavior.

Figure 36 is a plot of breakdown voltage, vs. gap spacing when the anode is plane and the cathode has a radius of one of three different curvatures (0.200 inch, 0.062 inch, and a machined "point"). Figure 37 is obtained from the same data, but shows RF output versus gap spacing. The supply voltage was either steady, or pulsed from a supply having a rise time of the order of 100 nanosec. It can be seen that the use of pulsed voltage raises the effective hold-off voltage of a given gap by a factor of as much as 2 or 3. This result is in accord with theory. The "statistical time" (or "waiting period") of the gap may be effectively somewhat greater than 100 nanosec., so that the gap simply does not have time to respond during the period of voltage rise. This behavior is desirable because, as will be seen later, the rise time (which follows the "waiting period") is not adversely affected and the RF output is

indeed correspondingly improved. From Fig. 36, one might also conclude that a more-pointed cathode leads to a higher hold-off voltage. This observation runs counter to expectation. Possibly the data involving this parameter are imprecise due to the effects of misalignment. In addition, when the radius of curvature is so large compared to the gap (and even the "pointed" cathode is quite blunt under the magnifying glass) the effects of radius may be less than the effects of surface finish, local temperature, etc. Finally, there may be additional effects in that the pointed shape couples more effectively to the RF field, as discussed in Section IIA4.

The electrode material used here was a tungsten matrix impregnated with copper. For the data of Figs. 36 and 37, the particular material was 57% tungsten, 43% copper. In Fig. 38, we compare the results using this material with results using 70% tungsten and 30% copper. For 70/30 material, breakdown voltages (steady and pulsed) were observed to be halved. With a steady applied voltage, however, one would not expect such a difference, since "statistical time," which is the only parameter dependent on work function, is not involved. Perhaps the alloy with more copper runs cooler, while erosion and work function are less important at the voltages used. More testing is needed, and with other materials. Moreover, the effect of the electrode material on rise time may outweigh its effect on voltage alone.

Corresponding to the variation of firing voltage with gap spacing, the approximate rise times in the range 0.3 to 2.5 nanosec. were noted. The trend, as expected, is for the rise time to increase substantially with spacing for spacings greater than about 0.008 inch. (Below 0.008 inch, the data would not be expected to be very reliable.) Also, as expected, there is no significant

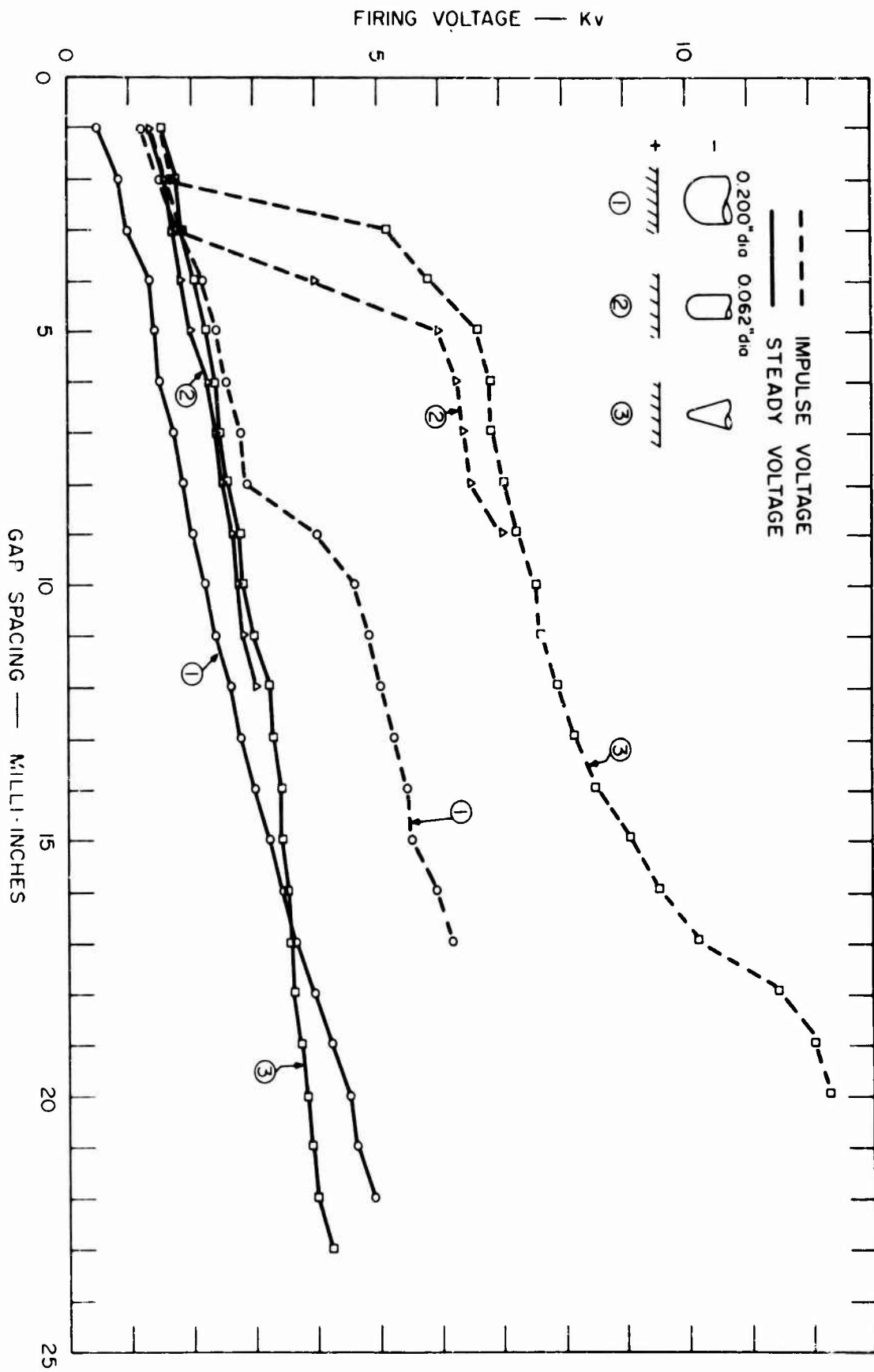


Fig. 36 Breakdown Voltage vs. Gap Spacing

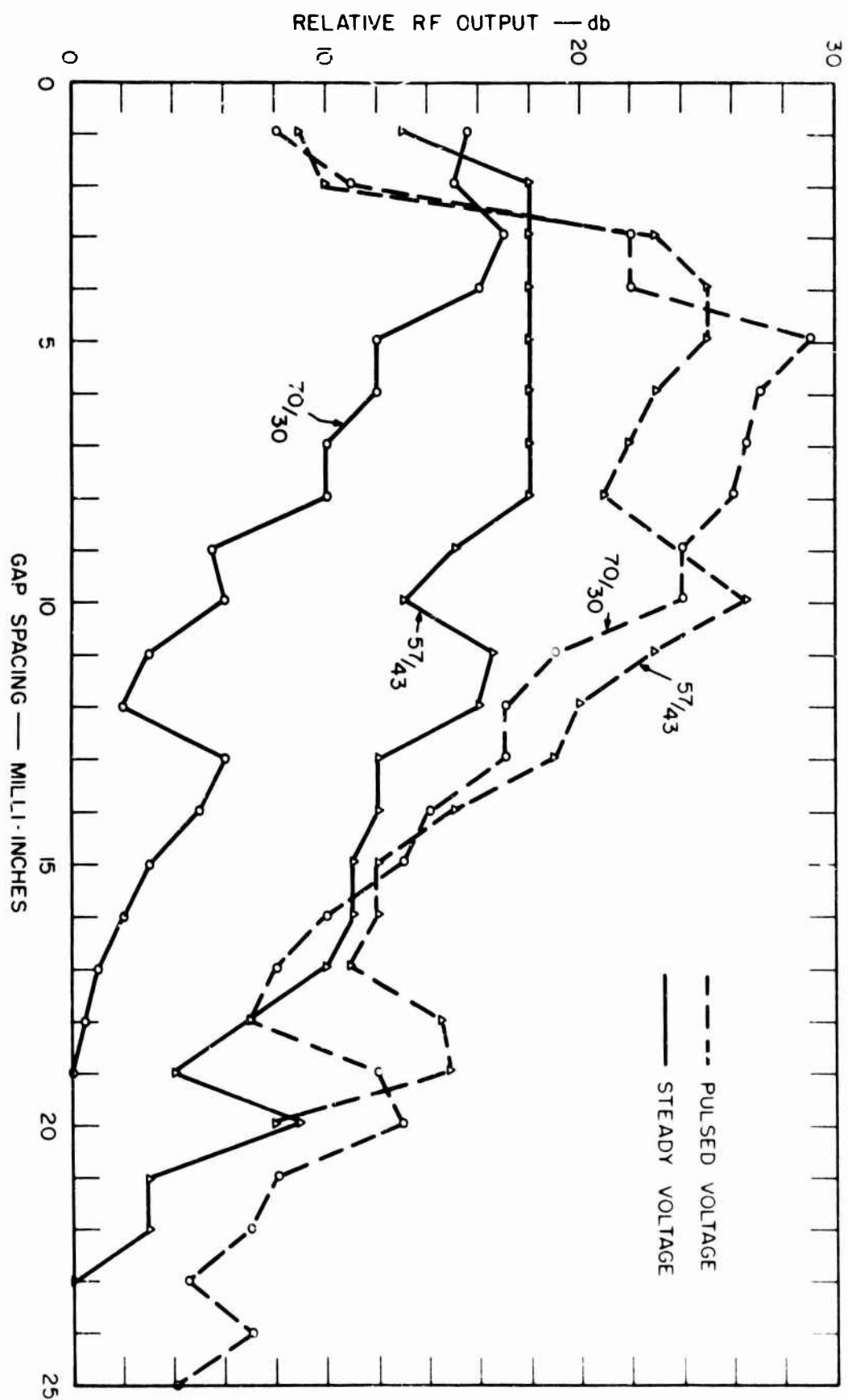


Fig. 38 RF Output vs. Gap Spacing for Different Materials



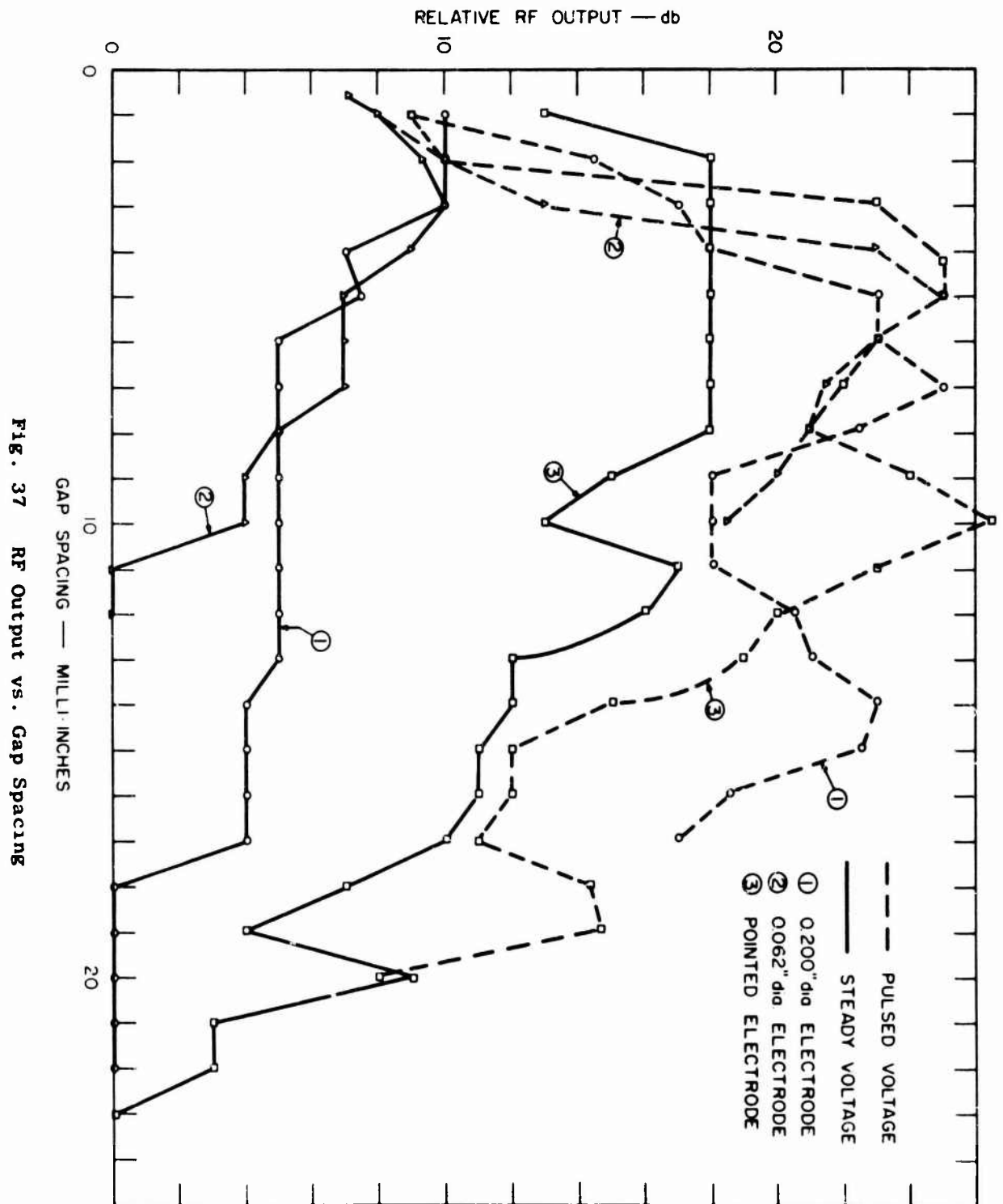


FIG. 37 RF Output vs. Gap Spacing

difference in rise times due to pulsed voltage as opposed to d-c voltage. There is an indication that the more pointed cathode usually leads to shorter rise times at a given spacing. At this time, though, the voltage is also higher. In the atmospheric gap, the rise time can be kept below 1 nanosec. only for gaps shorter than 0.010 inch, for which the firing voltage would not be more than about 4 kilovolts steady, or about 8 kilovolts pulsed.

Plotting relative RF output vs. gap spacing (Figs. 37 and 38) indicates the combined effects of voltage and rise time: The output increases at first because the rising voltage matters most, but ultimately the output falls because the effects of increasing rise time outweigh the effects of voltage. The advantages of the pointed cathode, which did reveal shorter rise times and (unaccountably) higher voltages, show up in augmented RF output at least with a steady voltage. The 2- to 3-fold increase of firing voltage at a given spacing, due to pulsing the voltage, should theoretically give 6 to 9 db more RF output if rise times are unaffected. Figures 37 and 38 do indeed show effects of this order.

In Figs. 39 and 40, where firing voltage is the abscissa, we are strongly reminded that in a practical gap at microwave frequencies, the RF output cannot be expected to increase indefinitely as the square of the firing voltage. The effects of the different electrode alloys (Fig. 40) may well be due to surface textures or degree of bluntness of the point rather than to a parameter like work function or thermal conductivity.

The correlation between spark rise time and RF output, for a representative case, appears strikingly in Fig. 41. The data have a strong downhill slope. Since voltage is not constant for this plot, it might be more appropriate to

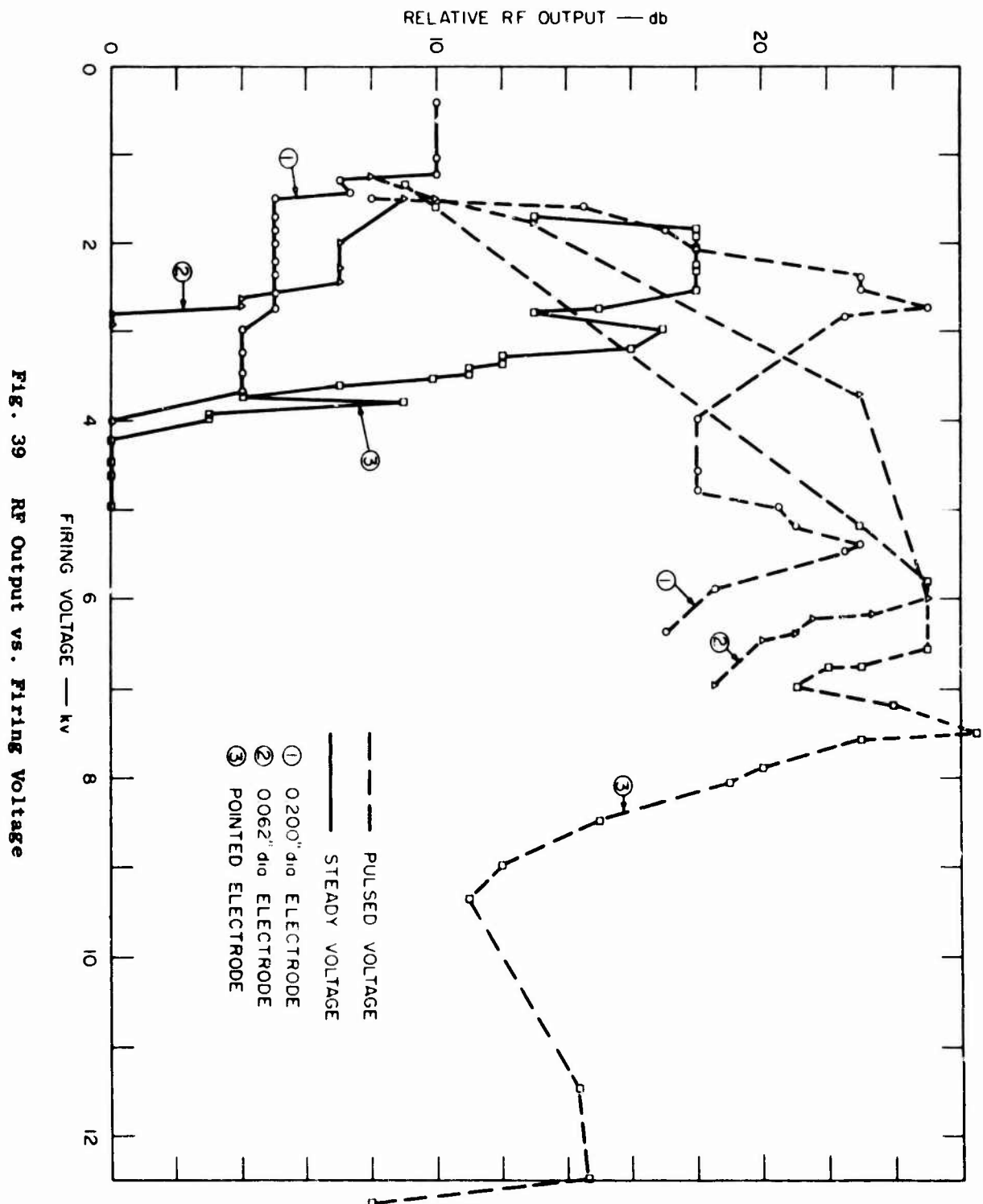


Fig. 39 RF Output vs. Firing Voltage

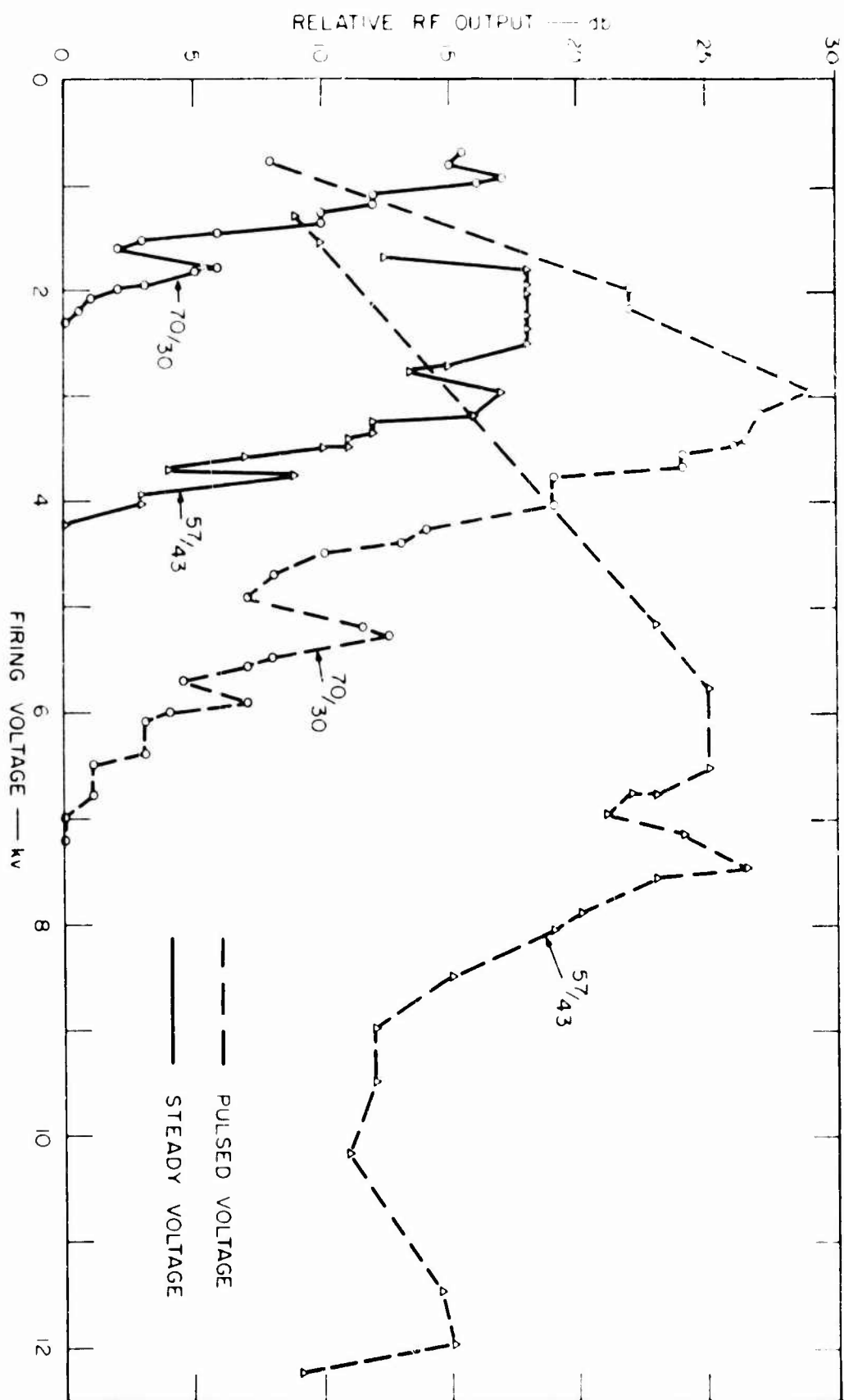


FIG. 40 RF Output vs. Firing Voltage for Different Materials

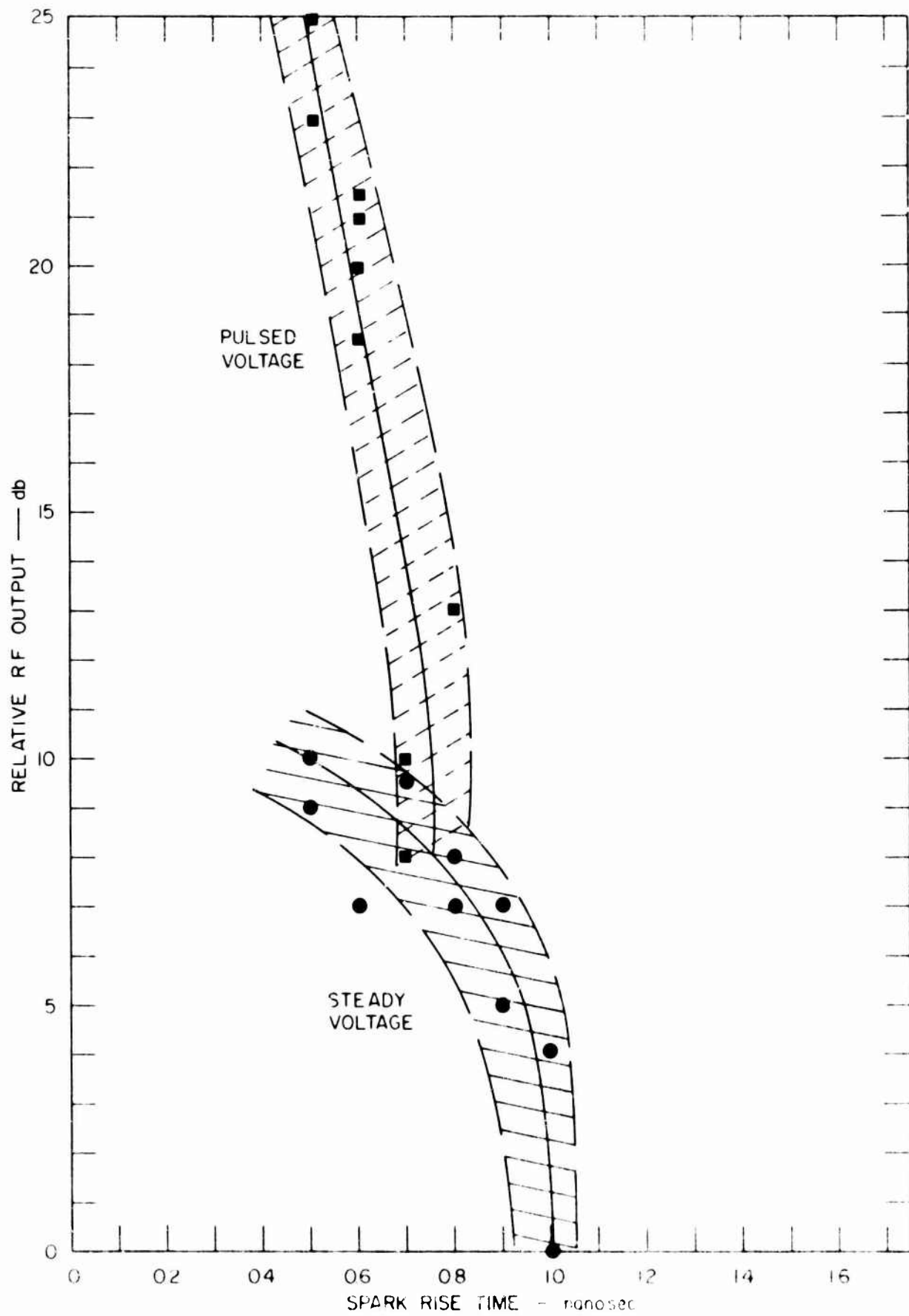


Fig. 41 RF Output as a Function of Firing Time

normalize out the variable voltage by plotting RF output divided by the square of the firing voltage. Since voltage is generally increasing with rise time (and gap spacing) for a given shape of point, the revised plot would show downhill runs of even greater slope. At the frequency of operation (2410 Mc) one indeed pays a heavy penalty for finite rise time.

Much more work is needed to elaborate the results obtained here, and to extend the investigation to other electrode materials. The work reported, however, does make clear the interdependence of the various factors and emphasizes once again the importance of studying the total behavior of the system as a function of its design parameters.

### III CONCLUSIONS AND RECOMMENDATIONS

The work done under this program demonstrates the capability of using a spark gap to generate short pulses of microwave frequencies of controllable shape. Operating at relatively low voltages (less than 4000 volts with the dc supply) we have demonstrated the capability of obtaining pulses a few tens of nanoseconds in width having up to 50 watts of power.

This demonstration indicates the need for a continuation of the work to determine the ultimate capability of this type of device for high-power short-pulse generation. Work so far has been concerned with the development of the necessary techniques and with the identification and elucidation of the principles involved. Only as qualitative understanding has been obtained have we been able to determine the designs that should be studied and the measurements that will give us the quantitative understanding necessary for a final evaluation.

The next phase of the study should include the following:

- (1) Device design: The next phase of the work should be based primarily on the Mod IV design, such as is illustrated in Fig. 10 or 34. This type of design may not prove to be the one of ultimate interest since the pulse it generates has an exponentially decaying tail. For purposes of evaluation, however, it is useful because of its simplicity and controllability.

To give the flexibility necessary for a thorough evaluation, it will be necessary to consider the effects of various modifications of the geometry. What happens if we vary the diameter of the center conductor? Or should the center conductor be conical or spherical? Should the outer conductor also be conical or spherical?

These different geometries can be studied by a combination of theory and cold-test measurements. The results can be given in terms of the Q's and impedances. These figures will then provide quantitative data for interpreting the results in operating models.

- (2) Spark-gap design: Intensive work should be done on the effect of various likely modifications of the spark-gap environment.

The modifications studied should include:

- (a) High pressure. It is probably premature, at this point, to consider going to pressures of hundred of atmospheres, but measurements should be made under moderately high pressures of tens of atmospheres.
- (b) Gas composition. The question of whether we want a gas with a low or high ionization potential should be investigated. The effect of the presence of gases such as water, or sulfur hexafluoride, which have a large electron-capture cross-section should also be considered. In all cases the evaluation should be made in terms of the RF conversion conductance with the gap and voltage adjusted for maximum output.
- (c) Liquid dielectric. We should measure what can be accomplished by flooding the gap with a liquid dielectric of high break-down strength.
- (d) Dielectric tape. One very interesting possibility is to introduce a disposable dielectric tape into the gap. The tape could be an oil-impregnated paper, or it could itself be a dielectric material such as Mylar. The tape would be pulled through the gap at such a rate that each firing would be through a virgin section of the tape.



- (e) Electrode materials. We have noted what appears to be a significant variation of the behavior with electrodes of 54/46 and 70/30 copper-impregnated tungsten-matrix material. This work should be carried further to see if substantial improvement can be obtained with other materials. We have also noted the possibility of using a mercury-wetted electrode surface which offers a renewable surface to the discharge.
- (f) Vibratory gap. The possibility of imposing a mechanical vibration on the gap has been noted. It is expected to offer some distinct advantages in terms of stability and (perhaps) life. It might be particularly advantageous in connection with a disposable tape.
- (3) Power application: There appears to be a substantial advantage in using a pulsed supply--as one would expect. The use of an ordinary radar modulator with a rise time of the order of 100 nanoseconds or more gave an improvement by a factor of 2 to 3. A faster rising pulse should give a substantial further improvement.
- (4) Theoretical: We have inferred, indirectly, the importance of what we have called the transient impedance of the discharge. This should be investigated theoretically. It is not clear how one might measure the transient impedance directly, but it would be interesting and instructive to compute the effects of various assumed behaviors. Such computations might prove to be of great importance in recognizing the significance of experimental results and in making meaningful any inference regarding ultimate capability.

This work in general should be done at reasonably high but not super-high voltages (several tens of kilovolts, but not megavolts). The work should be done at a frequency that is not so high as to preclude instantaneous measurements with modern equipment, but high enough to be well within the microwave range. S-band seems to be a suitable compromise.

The results of this work should establish the capability of this type of device at intermediate power levels, and should permit a realistic inference as to what might be accomplished at the limits of existing technology.

## APPENDIX A

### ANNOTATED BIBLIOGRAPHY OF SPARK-GAP TECHNOLOGY

1. Adlam, J.H. and L.S. Holmes, "Production of Millimicrosecond Current Pulses Using a Pressurized Spark Gap," Journal of Scientific Instruments, 37, 385-8, (October 1960)

Discusses constructions of a triggered, pressurized (150 psi) spark gap producing pulses of 10,000 amp at 4.5 ns. Apparatus discharges a number of charged coaxial cables in parallel.

2. Broadbent, T.E. and A.H.A. Shlash, "The Hot-Wire Triggered Spark Gap at Very High Voltages," British Journal of Applied Physics 13, 396-7 (December 1962)

Indicates that presence of hot-wire trigger embedded in surface of spark gap member tends to lower gap breakdown voltage.

3. Cormack, G.D. and A.J. Barnard, "Low-Inductance Low-Pressure Spark Gap Switch," The Review of Scientific Instruments 33, 606-10 (June 1961)

Discussion of a triggered "crowbar" switch operating at up to 25 kv with currents of up to 500,000 amp.

4. Durnford, J. and N.R. McCormick, "The Production of Current Pulses by Means of a Chopped Discharge," Proceedings of the IEE 99, Part II, 33-7 (February 1952)

Illustrates a scheme for developing relatively steep-sided, flat-topped current pulses of up to 500 amp by chopping the main gap current with a second triggered spark gap.

5. Fischer, J., "High Voltage Pulse Probe of Fast Rise Time for Spark Chambers," Review of Scientific Instruments 35, 125-6 (January 1964)

Technical note on a 25-kv probe to provide undistorted voltage division on pulses with rise times down to 2 ns.

6. Fletcher, R.C., "Production and Measurement of Ultra-High Speed Impulses," The Review of Scientific Instruments 20, 861-9 (December 1949)

Definitive paper on generation of pulses with rise times down to 0.4 ns. Discusses problems in impedance matching for observation on oscilloscope. Unfortunately, paper predates the high speed sampling-type oscilloscope.

7. Hagerman, D.C. and A.H. Williams, "High-Power Vacuum Spark Gap;" The Review of Scientific Instruments 30, 182-3 (March 1959)

Discussion of a 75-kv vacuum (0.5  $\mu$  Hg) spark gap. Lifetime between maintenance periods measured in hundreds of shots.

8. Johnstone, J.H., "The Spark Gap--New Circuit Component," Tele-Tech & Electronic Industries 15, 80 (August 1956)

9. Levy S., "Spark Gap Studies," Report on D.A. Subtask No. 1G6-22001-A-055-02-24, U.S. Army Electronics Research and Development Laboratories, Fort Monmouth, New Jersey.

Progress report on continuing study of spark gap application to radar modulators. Specific items covered are electrode erosion and triggering filter.

10. Little, R.P. and S.R. Smith, "Electrical Breakdown in Vacuum," IEEE Transactions on Electron Devices ED-12, 77-83 (February 1965)

Discusses undesirable aspects of electrical breakdown as it occurs in vacuum tubes, vacuum capacitors, etc.

11. McFarlane, H.B., "Spark Gaps for Fast High-Voltage Switching," Electronics 72-3 (31 July 1959)

Discusses uses of commercial spark gaps for high-speed switching.

12. Olson, W., "Treat Spark Gaps as components," Electronic Industries 78-9 (November 1958)

Inconclusive paper on spark gaps as protective devices.

13. Smith, O.E., "Improved High-Voltage Spark Gap, Requiring Zero Energy to Trigger," The Review of Scientific Instruments 35, 134 (January 1964)

14. Theophanis, G.A., "Millimicrosecond Triggering of High-Voltage Spark Gap," The Review of Scientific Instruments 31, 427-32 (April 1960)

Extensive discussion of triggering and synchronizing spark gap discharges.

15. McDonald, D.F., C.J. Benning and S.J. Brient, "Subnanosecond Risettime Multikilovolt Pulse Generator," The Review of Scientific Instruments 36, 504 (April 1965)

A recent study of slow and fast gaps in series. The discharge of the slow gap causes a large overvoltage to appear across the fast gap within an interval of time that is short compared to the time spent, on the average, waiting for a triggering event to occur.

## APPENDIX B

### REFERENCES

1. Hellar, M.W., Jr., and W.G. Holter, "A Transmission Line Oscillatory Pulse Generator," Proc. National Electronics Conference, 9, 161-170 (1953).
2. Ramsay, J.F., "Microwave Antenna and Waveguide Techniques before 1900," Proc. IRE, 46, 405-415 (February 1958).
3. Dolphin, L.T. Jr. and A.F. Wickersham, Jr., "Modern Spark Transmitter Techniques," SRI Final Report, Project 4548, Contract Nonr-4178(00), Stanford Research Institute, Menlo Park, California (December 1964).
4. Hart, J. "Production of Millimeter Waves by a Spark Generator," J. Appl. Phys. 29, 743 (1958).
5. Saxton, W.A. and H.J. Schmitt, "Transients in a Large Waveguide," Proc. IEEE 51, 405-406 (February 1963).
6. Potok, M.H.N., "A Critical Review of Researches into Millimetric-Wave Sparked Generators," J. Brit. Institute of Radio Engineers 13, 490 (1953).
7. Farrands, J.L., "The Generation of Millimeter Waves," Inst. EE Proc. 102C, 98-103 (March 1955).

in the understanding of the process, it is not sufficient to study the different components separately. It is instead, of paramount importance to study in detail the performance of the system as a functioning whole.

It is concluded that the use of spark gaps for the generation of short pulses at microwave frequencies is well worth further exploration.

UNCLASSIFIED

Security Classification

DOCUMENT CONTROL DATA - R&D		
(Security classification of title, body of abstract and in-issuing annotation must be entered when the overall report is classified)		
1 ORIGINATING ACTIVITY (Corporate author)		2a REPORT SECURITY CLASSIFICATION
Stanford Research Institute Menlo Park, Calif.		Unclassified
		2b GROUP
3 REPORT TITLE		
Energy Conversion Techniques for Microwave Generation		
4 DESCRIPTIVE NOTES (Type of report and inclusive dates)		
Final Report, March 1964-May 1965		
5 AUTHOR(S) (Last name, first name, initial)		
Pease, M. C.		
6 REPORT DATE	7a TOTAL NO OF PAGES	7b NO OF REFS
August 1965	110	28
8a CONTRACT OR GRANT NO. AF30(602) -3368		9a ORIGINATOR'S REPORT NUMBER(S)
b. PROJECT NO. 4506		4913
c. Task No. 450603		9b OTHER REPORT NO(S) (Any other numbers that may be assigned this report)
d		RADC-TR-65-254
10. AVAILABILITY/LIMITATION NOTICES		
Qualified requestors may obtain copies of this report from DDC. Release to CFSTI is authorized.		
11. SUPPLEMENTARY NOTES		12 SPONSORING MILITARY ACTIVITY
		Rome Air Development Center Griffiss AFB NY 13442
13 ABSTRACT		
<p>The purpose of this contract was the study and evaluation of the feasibility of using unconventional methods for the generation of high-power short pulses of microwave energy. For this purpose, converters were studied using spark gaps operating in various types of microwave structures.</p> <p>In Section II-A, the general design principles are discussed in considerable detail that have emerged from this study. In Section II-B, it is recognized that the use of spark gaps for RF generation is generically related to the devices used by early workers, and to certain devices currently being studied for sub-microwave operation. A survey of some of the more notable steps in the historical development of such devices is included. In Section II-C, the actual work done under this contract is described in some detail, and the evidence confirming the principles detailed in Section II-A is recounted. In Section III, detailed recommendations for further work are given.</p> <p>The work, in general, demonstrates that spark gaps can be used for the generation of short (e.g. 100 periods) pulses of microwave energy. It also demonstrates that this method of generating power does require very careful attention to the integrated design of the spark gap and its associated microwave and driving circuitry. The interactions between the spark gap and both the microwave circuitry and the driving circuitry are, in some cases, quite subtle. At this stage</p>		

DD FORM 1473

JAN 64

UNCLASSIFIED

Security Classification

UNCLASSIFIED

Security Classification

14 KEY WORDS	LINK A		LINK B		LINK C	
	ROLE	WT	ROLE	WT	ROLE	WT
Microwave Hertz Oscillator Spark Gap High Power Nanosecond Pulses						

## INSTRUCTIONS

1. **ORIGINATING ACTIVITY:** Enter the name and address of the contractor, subcontractor, grantee, Department of Defense activity or other organization (corporate author) issuing the report.

2a. **REPORT SECURITY CLASSIFICATION:** Enter the overall security classification of the report. Indicate whether "Restricted Data" is included. Marking is to be in accordance with appropriate security regulations.

2b. **GROUP:** Automatic downgrading is specified in DoD Directive 5200.10 and Armed Forces Industrial Manual. Enter the group number. Also, when applicable, show that optional markings have been used for Group 3 and Group 4 as authorized.

3. **REPORT TITLE:** Enter the complete report title in all capital letters. Titles in all cases should be unclassified. If a meaningful title cannot be selected without classification, show title classification in all capitals in parenthesis immediately following the title.

4. **DESCRIPTIVE NOTES:** If appropriate, enter the type of report, e.g., interim, progress, summary, annual, or final. Give the inclusive dates when a specific reporting period is covered.

5. **AUTHOR(S):** Enter the name(s) of author(s) as shown on or in the report. Enter last name, first name, middle initial. If military, show rank and branch of service. The name of the principal author is an absolute minimum requirement.

6. **REPORT DATE:** Enter the date of the report as day, month, year, or month, year. If more than one date appears on the report, use date of publication.

7a. **TOTAL NUMBER OF PAGES:** The total page count should follow normal pagination procedures, i.e., enter the number of pages containing information.

7b. **NUMBER OF REFERENCES:** Enter the total number of references cited in the report.

8a. **CONTRACT OR GRANT NUMBER:** If appropriate, enter the applicable number of the contract or grant under which the report was written.

8b, &, & 8d. **PROJECT NUMBER:** Enter the appropriate military department identification, such as project number, subproject number, system numbers, task number, etc.

9a. **ORIGINATOR'S REPORT NUMBER(S):** Enter the official report number by which the document will be identified and controlled by the originating activity. This number must be unique to this report.

9b. **OTHER REPORT NUMBER(S):** If the report has been assigned any other report numbers (either by the originator or by the sponsor), also enter this number(s).

10. **AVAILABILITY/LIMITATION NOTICES:** Enter any limitations on further dissemination of the report, other than those

imposed by security classification, using standard statements such as:

- (1) "Qualified requesters may obtain copies of this report from DDC."
- (2) "Foreign announcement and dissemination of this report by DDC is not authorized."
- (3) "U. S. Government agencies may obtain copies of this report directly from DDC. Other qualified DDC users shall request through \_\_\_\_\_."
- (4) "U. S. military agencies may obtain copies of this report directly from DDC. Other qualified users shall request through \_\_\_\_\_."
- (5) "All distribution of this report is controlled. Qualified DDC users shall request through \_\_\_\_\_."

If the report has been furnished to the Office of Technical Services, Department of Commerce, for sale to the public, indicate this fact and enter the price, if known.

11. **SUPPLEMENTARY NOTES:** Use for additional explanatory notes.

12. **SPONSORING MILITARY ACTIVITY:** Enter the name of the departmental project office or laboratory sponsoring (paying for) the research and development. Include address.

13. **ABSTRACT:** Enter an abstract giving a brief and factual summary of the document indicative of the report, even though it may also appear elsewhere in the body of the technical report. If additional space is required, a continuation sheet shall be attached.

It is highly desirable that the abstract of classified reports be unclassified. Each paragraph of the abstract shall end with an indication of the military security classification of the information in the paragraph, represented as (TS), (S), (C), or (U).

There is no limitation on the length of the abstract. However, the suggested length is from 150 to 225 words.

14. **KEY WORDS:** Key words are technically meaningful terms or short phrases that characterize a report and may be used as index entries for cataloging the report. Key words must be selected so that no security classification is required. Identifiers, such as equipment model designation, trade name, military project code name, geographic location, may be used as key words but will be followed by an indication of technical context. The assignment of links, rules, and weights is optional.

UNCLASSIFIED

Security Classification